

**Ad-atoms and Their Enhancement Effects on Pt
Activity for Formic Acid Oxidation**

by

Muhammad Akhtar Khan

A thesis submitted to the School of Graduate Studies in partial fulfillment of the
requirements for the degree of

Master of Science

Department of Chemistry

Memorial University

St. John's, Newfoundland

May, 2016

Abstract

Formic acid oxidation has been widely studied at Pt as a model reaction to understand fundamental aspects of electrocatalytic reactions in fuel cells. Electrocatalytic oxidation of formic acid takes place through two parallel pathways (direct and indirect). The indirect pathway proceeds via CO as an intermediate, which is known to be responsible for the poisoning of Pt and its consequent decrease in activity. Surface modification of Pt with ad-atoms is known to hinder this poisoning and promote the direct pathway. The incorporation of polymers (polyaniline, polycarbazole, polyindole) as supports also increases activity. Irreversibly adsorbed Sb and Bi on Pt are known to show high electrocatalytic activity for formic acid oxidation. This work presents the dependence of Sb and Bi irreversible adsorption on immersion time, metal solution concentration and pH. The activity of Sb and Bi modified Pt was correlated against immersion time and percent coverage of Pt by ad-atoms. Polyaniline support effects in combination with a Bi modified Pt catalyst showed enhancement in oxidation current compared to Pt-Bi.

Acknowledgements

I would first like to express my sincere gratitude to my supervisor Dr. Peter Pickup for his continuous support throughout my program. His patience, motivation, enthusiasm and immense knowledge have made my MSc an enjoyable and unforgettable experience. I could not have asked for a better advisor for my program.

I would like to thank my supervisory committee, Dr. Bob Helleur and Dr. Peter Warburton for the advice, support and time they have dedicated throughout my program.

I acknowledge the support staff especially the staff members of C-CART and the technicians working out of the Department of Chemistry. I would also like to thank the administration and physical science store staff for their help.

I would like to extend my sincere gratitude to the funding agencies that made my program possible: School of Graduate Studies, the Chemistry Department and NSERC.

Contents

Abstract	ii
Acknowledgements	iii
List of Figures	vi
List of Abbreviations	x
List of Symbols	xii
1 Introduction.....	2
1.1 Fuel cells	2
1.1.1 History and rationale behind fuel cell development	2
1.1.2 Commercialization challenges	6
1.1.3 What is a fuel cell?.....	7
1.1.4 Working principle	7
1.1.5 Classification of fuel cells.....	8
1.2 Why direct proton exchange membrane fuel cells (PEMFCs)?.....	9
1.3 Direct formic acid fuel cells (DFAFCs).....	9
1.3.1 Why formic acid?.....	9
1.4 DFAFC electrochemistry and electro-oxidation mechanism at Pt and Pd.....	12
1.5 Ad-atoms	17
1.5.1 Surface modification approaches by ad-atoms	18
1.5.2 Theoretical justification of ad-atoms modification for catalysis	19
1.5.3 Pt based surface modified catalysts	22
1.6 Polymer supports for DFAFC catalysts	23
1.7 Research objectives	25
1.8 References	26
2 Experimental.....	42
2.1 Chemicals	42
2.2 Synthesis of Pt nanoparticles (NP).....	42
2.3 Preparation of working electrodes.....	42
2.4 Instrumentation.....	43
2.5 Voltammetric experiments	43

2.6	References	45
3	Sb ad-atoms and their enhancement effects on Pt activity for formic acid oxidation	47
3.1	Introduction	47
3.2	Results and Discussion.....	49
3.2.1	Determination of surface area of the platinum nanoparticles (Pt NP)	49
3.2.2	Oxidation of formic acid.....	52
3.2.3	Oxide formation and stability of Sb ad-atoms	54
3.2.4	Dependence of Sb coverage on immersion time.....	57
3.2.5	Formic acid oxidation: cyclic voltammetry	59
3.2.6	Dependence of formic acid oxidation activity on Sb coverage	63
3.2.7	Long-term activity test: chronoamperometry	64
3.3	Conclusions	66
3.4	References	67
4	Electroactivity of PANI supported Pt modified by Bi ad-atoms	72
4.1	Introduction	72
4.2	Results and Discussion.....	74
4.2.1	Characterization of CVs of Bi modified Pt NP and Bi ad-atom stability	74
4.2.2	Electroactivity of Bi modified Pt versus immersion time.....	79
4.2.3	Electroactivity of Pt modified by ad-atoms for formic acid oxidation	86
4.2.4	Optimum metal solution concentration for adsorption of Bi over Pt NP	87
4.2.5	Constant potential evaluation of Bi modified Pt for formic acid oxidation.	88
4.2.6	Formic acid oxidation by Pt NP modified by (Bi + Sb)	90
4.2.7	PANI support effect for Pt and Bi modified Pt for formic acid oxidation...	91
4.3	Conclusions	96
4.4	References	98
5	Summary and Future Work	104

List of Figures

- 3.1 Cyclic voltammogram (100 mV s^{-1}) of a GC/Pt (Pt NP = $0.64 \mu\text{g}$) electrode in $0.1 \text{ M H}_2\text{SO}_4$52
- 3.2 Voltammogram (10 mV s^{-1}) of GC/Pt (Pt NP = $0.64 \mu\text{g}$) electrode in $0.1 \text{ M H}_2\text{SO}_4 + 0.5 \text{ M HCOOH}$ 53
- 3.3 Voltammograms (100 mV s^{-1}) of GC/Pt (Pt NP = $0.64 \mu\text{g}$) electrode that had been immersed in $0.1 \text{ mM Sb}_2\text{O}_3 + 0.1 \text{ M H}_2\text{SO}_4$ for 1 min.....55
- 3.4 Voltammograms (100 mV s^{-1}) of GC/Pt (Pt NP = $0.64 \mu\text{g}$) and GC/Pt electrodes modified by immersion in $0.1 \text{ mM Sb}_2\text{O}_3 + 0.1 \text{ M H}_2\text{SO}_4$ for 30 min.....56
- 3.5 Voltammograms (100 mV s^{-1}) of GC/Pt (Pt NP = $0.64 \mu\text{g}$) and GC/Pt electrodes immersed for x min in $0.1 \text{ mM Sb}_2\text{O}_3$ and tested in $0.1 \text{ M H}_2\text{SO}_4$57
- 3.6 Relationship between Sb ad-atom coverage and immersion time.....58
- 3.7 Anodic scans (10 mV s^{-1}) of GC/Pt (Pt NP = $0.64 \mu\text{g}$) and GC/Pt electrodes immersed for 30 min in $0.1 \text{ mM Sb}_2\text{O}_3$ and tested in $0.1 \text{ M H}_2\text{SO}_4 + 0.5 \text{ M HCOOH}$60
- 3.8 Anodic scans (10 mV s^{-1}) of GC/Pt (Pt NP = $0.64 \mu\text{g}$) and GC/Pt

	electrodes immersed for x min in in 0.1 mM Sb ₂ O ₃ and tested in 0.1 M H ₂ SO ₄ + 0.5 M HCOOH	61
3.9	Electroactivity for formic acid oxidation at 395 mV versus Sb coverage (%) over Pt (experimental curve) and experimental curve comparison with theoretical model curve (current versus ad-atom coverage curve for the case where the ad-atoms are assumed to be catalytically inert and the current is originated only from those substrate atoms which were protected from poisoning).....	63
3.10	Chronoamperometry at 100 mV for GC/Pt (Pt NP = 0.64 μg) and GC/Pt electrodes that has been immersed in 0.1 mM Sb ₂ O ₃ , tested in 0.1 M H ₂ SO ₄ + 0.5 M HCOOH.....	64
4.1	Cyclic voltammograms (100 mV s ⁻¹) of GC/Pt (Pt NP = 0.64 μg) and GC/Pt electrodes that has been immersed in 0.1 mM Bi ₂ O ₃ + 0.1 M H ₂ SO ₄ for 5 min, tested in 0.1 M H ₂ SO ₄	74
4.2	Cyclic voltammograms (100 mV s ⁻¹) of GC/Pt (Pt NP = 0.64 μg) electrode that has been immersed in 0.1 mM Bi ₂ O ₃ and tested in 0.1 M H ₂ SO ₄ at 100 mV s ⁻¹	75
4.3	Cyclic voltammograms (100 mV s ⁻¹) of GC/Pt (Pt NP = 0.64 μg) electrode that has been immersed in x min in 0.1 mM Bi ₂ O ₃ or 0.1 mM Sb ₂ O ₃ and tested in 0.1 M H ₂ SO ₄	76
4.4	Relationship between Pt coverage by Bi ad-atoms and immersion time...80	
4.5	Speciation of Bi(III) in acidic solution.....	81

4.6	Second anodic scan of voltammograms of GC/Pt (Pt NP 1.25 μL = 0.64 μg) electrodes that has been immersed for 5 min in 0.1 mM Bi_2O_3 dissolved in 0.1 M H_2SO_4 and 0.5 M H_2SO_4 and tested in 0.1 M H_2SO_4 + 0.5 M HCOOH at 10 mV s^{-1}	82
4.7	Second anodic scan of voltammograms (10 mV s^{-1}) of GC/Pt (Pt NP = 0.64 μg) electrodes that have been immersed for x min in 0.1 mM Bi_2O_3 dissolved in 0.1 M H_2SO_4 and tested in 0.1 M H_2SO_4 + 0.5 M HCOOH	83
4.8	% Coverage (Bi) vs electroactivity of Bi modified Pt.....	85
4.9	The electroactivity for formic acid oxidation versus coverage (%) of Pt by Bi and Sb ad-atoms.....	86
4.10	Second anodic scan of voltammograms (10 mV s^{-1}) of GC/Pt (Pt NP = 0.64 μg) electrodes that has been immersed for 5 min in x mM Bi_2O_3 dissolved in 0.1 M H_2SO_4 and tested in 0.1 M H_2SO_4 + 0.5 M HCOOH	88
4.11	Chronoamperometry at 100 mV for GC/Pt and GC/Pt electrodes immersed in x min in 0.1 mM Sb_2O_3 / 0.1 mM Bi_2O_3 and tested in 0.1 M H_2SO_4 + 0.5 M HCOOH	90
4.12	Second anodic scan of voltammograms (10 mV s^{-1}) of GC/Pt (Pt NP = 0.64 μg) and GC/Pt electrodes immersed for 30 min in 0.1 mM Bi_2O_3 , 0.1 mM Sb_2O_3 and 0.05 mM (Bi_2O_3 + Sb_2O_3) dissolved in 0.1 M H_2SO_4 and tested in 0.1 M H_2SO_4 + 0.5 M HCOOH	91

4.13	Cyclic voltammograms (100 mV s^{-1}) of GC/Pt and GC/PANI/Pt electrodes in $0.1 \text{ M H}_2\text{SO}_4$	92
4.14	Second anodic scan of voltammograms (10 mV s^{-1}) of GC/Pt and GC/PANI/Pt electrodes in $0.1 \text{ M H}_2\text{SO}_4 + 0.5 \text{ M HCOOH}$	93
4.15	Second anodic scan of voltammograms of GC/Pt, GC/PANI/Pt, Bi modified GC/Pt and Bi modified GC/PANI/Pt electrodes in $0.1 \text{ M H}_2\text{SO}_4 + 0.5 \text{ M HCOOH}$ at 10 mV s^{-1}	95

List of Abbreviations

AFC	Alkaline fuel cell
CP	Conjugated polymer
CUTE	Clean urban transport for Europe
CV	Cyclic voltammetry
DEMS	Differential electrochemical mass spectrometry
DFAFC	Direct formic acid fuel cell
DMFC	Direct methanol fuel cell
ECTOS	Ecological city transport energy project
EMF	Electromotive force
EMIRS	Electrochemically modulated infrared spectroscopy
FCV	Fuel cell vehicle
FTIR	Fourier transform infrared spectroscopy
HUPD	Hydrogen underpotential deposition
ICE	Internal combustion engine
IRAS	Infrared reflection absorption spectroscopy
LSV	Linear scan voltammetry

MCFC	Molten carbonate fuel cell
MEA	Membrane and electrode assembly
NP	Nanoparticles
PAFC	Phosphoric acid fuel cell
PANI	Polyaniline
PEM	Polymer electrolyte membrane / proton exchange rate
PEMFC	Proton exchange membrane fuel cell
PTFE	Polytetrafluoroethylene
SCE	Saturated calomel electrode
SHE	Standard hydrogen electrode
SOFC	Solid oxide fuel cell
STEP	Sustainable transport energy project
UPD	Underpotential deposition
XPS	X-ray photoelectron spectroscopy
XRD	X-ray diffraction

List of Symbols

μ micro

μA micro ampere

A ampere

E° standard potential

I current

kW kilowatt

M mole L^{-1}

min minute

mM milli molar

mV milli volt

s second

T time

V voltage (volts)

Wh watt-hour

CHAPTER 1

Introduction

1 Introduction

1.1 Fuel cells

1.1.1 History and rationale behind fuel cell development

Scientific work on fuel cells dates back to 1838 and Sir William Grove is credited with the fundamental research on a fuel cell [1, 2]. However, there is controversy in the literature about the inventor of the fuel cell. It is believed that the German chemist Christian Friedrich Schönbein published his scientific research work about a fuel cell in the Philosophical Magazine in the January issue of 1839. However, Grove is attributed for the fact that he introduced the concept of a hydrogen fuel cell by conducting a simple experiment involving two platinum electrodes immersed in a solution of sulphuric acid. The other ends of both electrodes were sealed in tubes containing hydrogen, oxygen and water. He observed a rise in the water level with the passage of current between the two electrodes. Grove named his experimental setup “a Gas Battery” [3, 4].

It is also believed that the principle of the fuel cell was discovered by Christian Friedrich Schönbein [1, 5]. “The term ‘fuel cell’ was first used some 50 years after Grove’s ‘gas battery’ by Mond and Langer in 1889, to describe their device which had a porous platinum black electrode structure, and used a diaphragm made of a porous nonconducting substance to hold the electrolyte” [6].

Fundamental research related to fuel cells such as the inverse process (electrolysis) dates back to 1800. Research on the interconnection of fuel cell components such as electrodes, electrolytes, oxidizing and reducing agents dates back to 1893 by Friedrich

Wilhelm Ostwald [2, 4]. In 1896, Willaim W. Jacques developed a fuel cell with practical applications. In 1921, Emil Baur developed the first molten carbonate cell and it was Jacques who developed the first high power systems of 1.5 kW and 30 kW in 1921 [2, 3]. Francis Thomas Bacon developed the first fuel cell to convert air and hydrogen directly into electricity. He also developed a fuel cell that was used in submarines in World War II [4]. Bacon's work was used to develop a fuel cell used by NASA in the "Apollo" spacecraft by a company called "Pratt and Whitney" [3, 7, 8].

In early 1900, it was realized that hydrogen could become a common fuel for energy production, like coal, and that the twentieth century would be the beginning of a new era of "Electrochemical Combustion". The forecast about fuel cells replacing fossil fuels, however, even now in the twenty-first century, has not yet been accomplished [3].

Since 1950, the use of Teflon (polytetrafluoroethylene) or PTFE made it possible to develop aqueous fuel cells with platinum electrodes in acidic eletrolytes and carbon electrodes in alkaline media. Hence, the original design of the fuel cell was changed in 1955 by Thomas Grubb as he used a membrane made of polystyrene sulphate as an electrolyte and his work was extended by Leonard Niedrach, who develop a catalyst by deposition of Pt on the membrane for the redox reaction of hydrogen and oxygen [3, 8].

As far as the history of the development and implementation of practical terrestrial applications of fuel cells is concerned, the first fuel cell applied for transportation was developed by General Motors in 1960 but only for experimental purposes. Later on in 1993, Ballard (a Canadian company) demonstrated that buses can be powered by polymer electrolyte (PEM) fuel cells. Following the above examples, the automobile industry was

revolutionized by a dream of new technology “the hydrogen economy”. Fuel cells powered vehicles for commercialization were thought to be on the horizon. A sizeable portion of automobile manufacturing company’s budgets were dedicated to the research and development to compete with rivals for the introduction of commercial vehicles powered by fuel cells. Although the commercialization of fuel cell powered vehicles has been began [9], it is largely a work in progress to be able to compete with fossil fuel driven vehicles [10, 11] mainly due to high cost [12].

There are serious benefits to the environment and economy through the development of alternative or renewable energy sources. There is a continuous increase in energy demand due to growing population and the staggering use of modern technologies. Major chunks of energy come from fossil fuels [13]. The dependence on a single source (fossil fuels) of energy is a precarious situation as a shortage could be disastrous for the modern industrialized world [1]. Moreover, fossil fuel combustion has adverse effects on the environment as it produces SO_x , NO_x , CO_2 and particulate matter. The production of hydrocarbons and NO_x increases the ozone level in the lower atmosphere causing detrimental health effects. Particulate matter is the major cause of several respiratory infections. Production of SO_x causes acid rain that is detrimental to plants [7]. The above described disadvantages of fossil fuels have directed significant research towards environment friendly energy sources [14].

Fuel cells are considered one of the environmental friendly technologies which are free from the production of green house gases (provided that the fuel used is from renewable resources) and particulate matter. Fuel cell driven machines possess higher

energy efficiency relative to fossil fuel driven machines [15] and low maintenance costs. Although fuel used in fuel cells may contain carbon, the carbon emissions can be compensated by the regeneration of the fuelstock if it is produced from sustainable resources [16]. Moreover, since fuel cells are energy production devices as opposed to energy storage devices like batteries [17], they can be used for local production of energy. Hence, fuel cells can be used for distributed power supply purposes to avoid the cost of transmission lines and line losses. Furthermore, fuel cells are superior to photovoltaics, micro turbines and wind turbines applied to distributed power generation systems as shown in the table 1.1 [5, 18].

	Engine:diesel	Turbine generator	Photo voltaics	Wind turbine	Fuel cells
Capacity range	500 kW-5 MW	500 kW-25 MW	1 kW-1 MW	10 kW-1 MW	200 kW-2 MW
Efficiency	35%	29-42%	6-19%	25%	40-60%
Capital Cost(\$/kW)	200-350	450-870	6600	1000	1500-3000
Operation & maintenance cost (\$/kW)	0.005-0.015	0.005-0.0065	0.001-0.004	0.01	0.0019-0.0153

Table 1.1. Comparison of fuel cells with other power generation systems [5, 18].

Commercially, fuel cells have incredible potential in the market for portable devices. Power sources for devices such as laptops, cameras, cell phones, radios, and power tools are required to have low cost, long run times, short response time, small size, long life and light weight [19] and a probable replacement of batteries by fuel cells has an estimated market value of £6bn and an overall global market potential of £13bn [16].

1.1.2 Commercialization challenges

Despite all of the above advantages, fuel cells have not been extensively commercialized [18, 20, 21]. There are a few hurdles to overcome for a wide range of commercialization such as cost, life time, durability and accessibility, although progress has been made in recent times [18, 22]. A major cost issue comes from the use of Pt as the main electrode material. We know that Pt is scarce and it is very expensive. To mitigate the issue of Pt cost, the use of nanoparticles (NP), making use of other metals to reduce the quantity of Pt and use of support materials such as polymers have been suggested [23]. The cost has been reduced from \$275/kW in 2002 to \$73/kW in 2008 [22] and furthermore to \$47/kW in 2012 [24]. It is still high relative to an internal combustion engine (ICE), which is the major rival of fuel cells for commercialization [22]. Other than cost, the durability of fuel cells is another major issue for commercialization with stability issues such as Pt agglomeration and Pt degradation [25]. Pt is also prone to poisoning by CO, H₂S, NH₃, and carbon-hydrogen compounds in the H₂ stream. Poisoning of Pt reduces the long term electroactivity of the catalyst which reduces the overall efficiency of the fuel cell. Furthermore, the stability issue that arises by the degradation of MEA (membrane and electrode assembly) limits long term use of fuel cells. Commercial usage for light weight vehicles requires 5000 hours of operation, over 4000 hours for stationary power generation and about 50,000 hours for portable technologies. Currently, most fuel cells can not go longer than a thousand hours of operation [22, 26].

Despite all of the above challenges, fuel cells are considered a viable option to replace ICEs in the transportation sector because they are a major consumer of fossil fuels

and hence a source of environmental pollution worldwide [27]. Fuel cells are superior relative to ICEs in performance, maintenance cost and running cost; although the initial price of a fuel cell is higher than an ICE. Therefore, fuel cells vehicles (FCVs) are costly compared to ICEVs [18]. It has been expected that the cost of FCVs will drop by 90% by 2020 and hence it is expected that FCVs will be mass produced [28]. CUTE (clean urban transport for Europe) [29], ECTOS (ecological city transport energy project) and Australian STEP (sustainable transport energy project) are a few examples of pilot projects using FCVs worldwide [22].

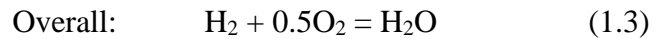
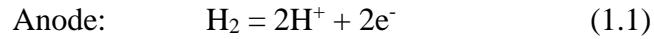
1.1.3 What is a fuel cell?

It is an electrochemical device that produces electrical energy by converting fuel into water, heat and other possible products. A fuel cell is an open thermodynamic system and it differs from a battery (a closed system) as it does not store reactants (fuel) or electrical energy, it does not need charging, and it can be used for an extended time period before replacement. A fuel cell converts chemical energy to electrical energy via an electrochemical process and it continues its operation provided that the fuel is continuously supplied and products are removed (usually water) [30, 31].

1.1.4 Working principle

A fuel cell consists of two electrodes (anode, cathode) and an electrolyte. The two electrodes are separated by an electrolyte to avoid a direct connection and it works as a membrane to transport ions selectively between the two electrodes. The anode is for oxidation and the cathode is for reduction. The fuel fed to the fuel cell chamber is oxidized at the anode and electrons pass via an external circuit to the cathode, where electrons and

oxidant combine to give water and heat (hydrogen fuel cell). The electrochemical reactions involved in a hydrogen fuel cell are given by the equation 1.1 to 1.3 [5, 18, 30]



1.1.5 Classification of fuel cells

Although the basic principle is the same, there are different types of fuel cells with differences in the fuel used, operating temperature, type of ions exchanged via the membrane, pressure and direct or indirect usage of the fuel. Fuel cells are conventionally classified on the basis of electrolyte and fuel. Presently, fuel cells are classified by the following five types

- 1) Alkaline fuel cells (AFC) with an alkaline solution electrolyte
- 2) Phosphoric acid fuel cells (PAFC) with acidic solution electrolyte
- 3) Proton exchange membrane fuel cell (PEMFCs) also known as polymer electrolyte membrane fuel cells
- 4) Molten carbonate fuel cells (MCFC) with molten carbonate salt electrolyte
- 5) Solid oxide fuel cells (SOFC) with ceramic ion conducting electrolyte in solid oxide form [5, 18, 24, 30]

1.2 Why direct proton exchange membrane fuel cells (PEMFCs)?

Direct fuel cells are a simplified type of fuel cell as fuel is fed directly without any reforming. For example, fuels such as formic acid, ethanol and methanol are fed directly into the fuel cell instead of reforming to hydrogen. Direct fuel cells are promising candidates for FCV and portable devices compared to fuel cells that require reformation of the fuel before it is introduced to the anode. Simplicity of design is handy for applications such as FCV and portable devices [32]. Furthermore, direct fuel cells have low operation temperatures which is favorable for applications in portable devices. Moreover, direct fuel cells have high power density, fast start up time, high efficiency, minimal corrosion problems, and easy and safe handling. Among fuel cells, the PEMFC is one of the best for applications in transportation and portable devices mainly due to their relatively low operational temperatures (≥ 100 °C) [33, 34]. Electrodes used in PEMFCs are made with the expensive noble metal Pt, which is susceptible to poisoning by impurities in the fuel or partial oxidation of fuel giving CO [35]. The high cost, loss of electroactivity of the Pt electrodes and breakdown of the PEM (polymer electrolyte membrane) are the impediments of PEMFCs for commercialization [24, 36].

1.3 Direct formic acid fuel cells (DFAFCs)

1.3.1 Why formic acid?

Since formic acid was proposed as a fuel for direct fuel cells, it has eclipsed a number of organic fuels such as methanol, ethanol, propanol, ethylene glycol, glycerol, formaldehyde, ethyl formate, dimethyl ether and dimethoxymethane [37]. Formic acid is promising relative to the above mentioned fuels due to its better oxidation kinetics, high

theoretical thermodynamic cell potential and relatively less fuel crossover [37, 38]. Formic acid also acts as an electrolyte by giving protons via its own dissociation [39, 40]. Furthermore, formic acid can be produced via renewable resources such as biomass and hydrogenation of CO₂, hence it results in low net emission of CO₂ to the environment [13].

The phenomenon of fuel diffusion fed to the anode compartment of a direct liquid fuel cell towards the cathode via the electrolyte membrane is known as fuel crossover [16]. Fuel crossover is a fundamental problem in DMFCs (direct methanol fuel cells). Methanol moves towards the cathode via the membrane because of diffusion (concentration gradient) and electro-osmotic drag/transport similar to the case of a water molecule bound to a proton [41, 42]. Fuel crossover causes loss of fuel, poisoning of the cathode (decomposition of fuel to CO), and reduction of the cathode potential (chemical short circuit) [16]. Formic acid has relatively low fuel crossover due to anionic repulsion between the Nafion membrane (sulfonic acid groups) and formate anions [16, 39].

Electro-oxidation of formic acid and methanol yields 2 and 6 electrons [16, 43]. The theoretical energy density of methanol is 4690 W h L⁻¹ while it is only 2086 W h L⁻¹ for formic acid. The lower energy density of formic acid relative to methanol can be compensated by using higher concentrations of formic acid as it has lower fuel crossover [44]. As methanol suffers from high fuel crossover, the maximum concentration that can be used is 2 M. However, formic acid can be used up to 20 M [45]. Moreover, formic acid has a higher theoretical electromotive force (EMF) than hydrogen or DMFCs calculated from the Gibbs energy [45-47]. Furthermore, methanol is a toxic (acidosis), volatile and flammable liquid. Toxicity of methanol is a serious issue for commercialization of DMFCs, as large volumes of methanol can be carried by CO₂ produced at the anode and exhausted

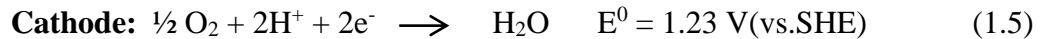
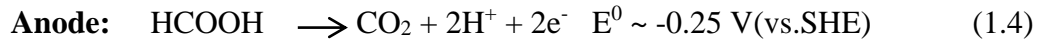
into the surroundings if used in portable devices [48, 49]. On the other hand, formic acid is a naturally occurring benign chemical, used as a food additive at lower concentrations [49] and its physical properties such as pungent smells and sour taste are handy to detect leakage or exposure [17]. Therefore, the usage of DFAFCs is advantageous relative to DMFCs in small power systems [47].

The major challenge for the commercialization of hydrogen fuel cells is the storage of hydrogen on board [50]. To compete with ICEs, hydrogen fuel cell driven vehicles need to meet the current driving range, performance and safety measures of ICEs. The efficiency of hydrogen fuel cells is 60% relative to ICE which is only ca. 25%. There is a large difference in the volumetric energy of hydrogen and petrol (5 kg of hydrogen is equivalent to 22 L of petrol) [51]. Hydrogen's volumetric energy density is about 3000 times less than gasoline. To resolve the issue of the large difference in the volumetric energy density between hydrogen and gasoline, and to compete in the commercial market, hydrogen has to be stored under high pressure at extremely low temperature as a liquid. To meet the goal of commercialization, the hydrogen storage system should have a specific energy density of 3.0 kWh kg⁻¹ and a cost of \$2 kWh⁻¹. However, current hydrogen storage technology does not meet these requirements [50].

Compared to the above mentioned challenges of cost, storage and safety concerns about hydrogen fuel cells, formic acid being a liquid at room temperature benefits from easy and uncomplicated transportation, refueling and safe handling. Hydrogen can be produced from formic acid or it (formic acid) can be used as fuel directly in DFAFCs with water and CO₂ as the only products [52].

1.4 DFAFC electrochemistry and electro-oxidation mechanism at Pt and Pd

A DFAFC is normally based on a PEMFC technology. It uses an air cathode where oxygen reduction is carried out via a four electron reaction, usually at a Pt based electrocatalyst. The direct oxidation of formic acid is a two electron process per molecule. Electrons are transferred via an external circuit to the cathode where they combine with oxidant (oxygen) to form water. Protons produced at the anode pass through the membrane (PEM) to the cathode [16, 17, 47, 53]. Formic acid electro-oxidation half reactions and overall reaction are described by equations 1.4 to 1.6 [47].

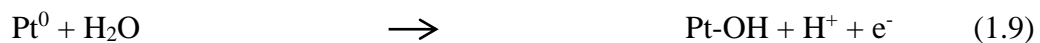


Formic acid has a dual pathway mechanism. The two pathways are classified as direct or indirect. In the direct pathway of electro-oxidation, formic acid is oxidized via a reactive intermediate [54-58]. In the indirect pathway, formic acid is first adsorbed onto the surface of the catalyst to form an intermediate adsorbed CO species through dehydration (poison formation). The adsorbed CO is then oxidized to CO₂. For the oxidation of adsorbed CO, an activated water molecule has to be adsorbed on a surface site nearby the adsorbed CO. For the adsorption of a water molecule on a surface site at an electrocatalyst, usually Pt, a high overpotential is required that is detrimental to the fuel cell efficiency [59-63]. The direct and indirect pathways of electro-oxidation of formic acid can be elaborated by equations 1.7 to 1.10 [58, 63-65].

Direct Pathway



Indirect Pathway



To find out the exact nature and structure of the adsorbed poisoning species in the indirect pathway of electro-oxidation of formic acid, several candidates were proposed such as CO, COH and CHO. Only CO was identified via spectroscopic (electrochemically modulated infrared spectroscopy EMIRS) analysis of the adsorbed poisoning species. CO can be detected by IR at 0.2 V and it completely vanishes at 0.7 V. It has been further confirmed by differential electrochemical mass spectrometry (DEMS) [66] and also by infrared reflection-absorption spectroscopy (IRAS) [55]. Hence, the detection of CO at low potential values indicates that it is the actual poisoning species. It is the poisoning species that causes the gradual loss of electroactivity of the electrocatalyst (Pt) and it is not the reactive intermediate for the direct electro-oxidation of formic acid [58, 66]. Moreover, the relationships between the rate of formation of poisoning species (CO) and its removal indicated that the contribution of the indirect pathway towards the faradic current was only 5% and this further substantiates that CO is the poisoning species [58].

For the direct pathway of electro-oxidation, candidates such as CHO, COOH and HCOO were suggested [58] with COOH being the most favorite [55]. However, COOH

was negated as being the reactive intermediate as it failed to be confirmed by spectroscopic techniques [61]. Adsorbed formate (HCOO) was detected on Pd, Ir, Pt [55] and chemically deposited Pt film electrode [61].

The role of adsorbed formate and whether it is solely responsible for the direct pathway of electro-oxidation of formic acid at Pt is also a point of debate [58, 61, 67, 68]. It was proposed that the rate of the direct pathway depends on the coverage of the electrocatalyst (Pt) surface and hence it (surface coverage) depends on CO free sites i.e., the less the blockage by poison (CO), the higher the coverage by formate and the greater the rate of the direct pathway [55]. However, in another study, it was proposed that formate is not only the intermediate for the direct pathway, it is also an intermediate for the indirect pathway [61, 68]. Therefore, the coverage of electrocatalyst (Pt) by formate is independent of blockage by CO [61].

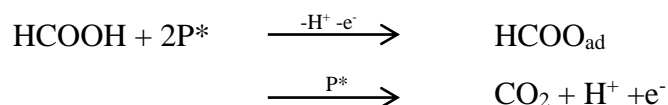
In contrast to the previous proposals about formate being an active intermediate, it has been proposed as a surface blocking species [58]. On the other hand, it has been proposed that formate disrupts the hydrogen bonding network at the water-metal interface and it creates an hydrophobic region. The hydrophobic region is conducive for the adsorption of formic acid in a C-H-down configuration. Hence, formate may be neither an active intermediate nor a surface blocking species. It may be a catalyst (adsorbed formate is conducive for the adsorption of formic acid that leads to oxidation) for formic acid oxidation [69].

In addition to the above contrary findings regarding the role of formate, it has been shown that the mechanism of formic acid oxidation depends on several factor such as pH, concentration of ionic species in the solution (formate, sulfate) and the presence of

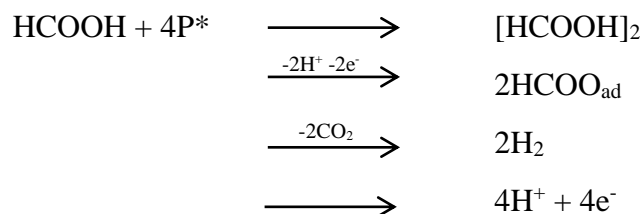
additional adsorbed species. Formic acid oxidation is generally conducted in sulfuric acid and adsorption of formate along with sulfate anions plays an important role in the overall mechanism. Adsorption of formate and sulfate are conducive to the adsorption of a second formate in a C-H down configuration. Moreover, the presence of other adsorbed ions such as bidentate formate stabilizes the surface configuration in the pH region of zero to two, which is conducive for formate adsorption in a C-H down configuration and its stabilization. At $\text{pH} > 5$, the adsorption of sulfate is probably absent and the overall oxidation current solely depends on the concentration of formate in the solution [70].

Due to the absence of spectroscopic evidence about COOH_{ads} [71] and the assumption that $-\text{COOH}$ is the reactive intermediate, the mechanism of formic acid electro-oxidation is still an unsolved puzzle [61]. A summary of mechanisms (dehydrogenation pathway) proposed is shown in scheme 1.1 [61].

Mechanism (I)

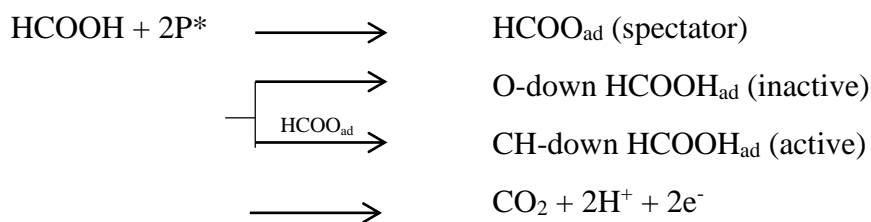


Mechanism (II)

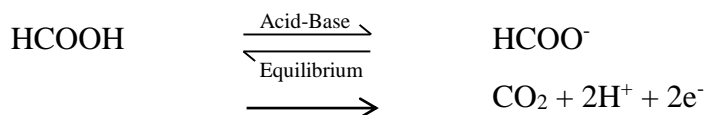


P^* represents the vacant metal surface site available for the reaction.

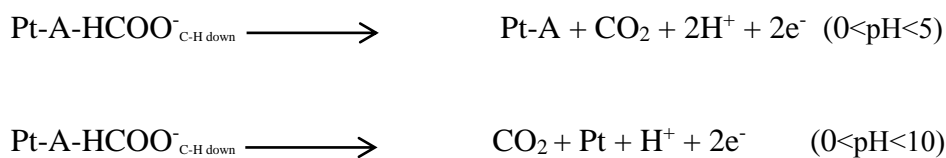
Mechanism (III)



Mechanism (IV)



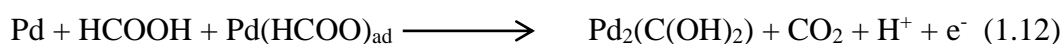
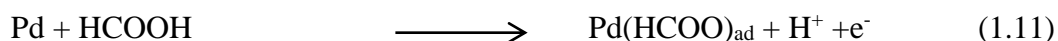
Mechanism (V) [70]



Scheme 1.1. Summary of proposed mechanisms (dehydrogenation pathway) of formic acid oxidation.

Electro-oxidation of formic acid at Pd proceeds almost entirely via a direct pathway [66], however the electroactivity declines over a period of hours of operation [15, 17, 61, 72]. Electro-oxidation of formic acid at Pd gives CO₂ at potential values corresponding to the hydrogen deposition region via the direct pathway and there are undetectable levels of CO (detection via Fourier transform infrared spectroscopy FTIR). The undetectable levels of adsorption of CO is mainly due to re-adsorption of CO₂ formed via the direct pathway. This indicates a much slower rate of poisoning of Pd relative to Pt. Probably the absorption

of species other than CO such as formate and bicarbonates could be the reason for slow poisoning leading to inactivity of Pd [73]. Intermediates such as bicarbonates [73] formed by disproportionation of intermediates of formic acid oxidation (formate) [74] may cause the slow decline of electroactivity and adsorption of intermediates can be depicted by the equations 1.11 to 1.13 [17].



Furthermore, aggregation of Pd NP, surface blockage by CO₂ bubbles, the presence of CO_{ad} [61], and adsorption of ions such as bisulfate are also implicated in the deactivation of Pd [72].

1.5 Ad-atoms

Electrocatalytic activity and selectivity of an electrocatalyst depends on the surface structure [75]. The surface structure of an electrocatalyst can be shaped to control the selectivity and activity, and hence to improve the electrocatalytic activity for a particular electrochemical reaction [59]. An electrocatalyst surface can be modified by adsorption of a submonolayer of noble metal atoms. Although the submonolayer adsorption of foreign ad-atoms is not stable and desorption might occur during the electrocatalytic reaction, it provides the advantage of recovery of the original surface and hence the same electrode material can be used to deposit ad-atoms of different metals for research purposes. Furthermore, ad-atoms can be deposited on localized facets of a crystalline electrocatalyst

surface to investigate the active sites for a particular electrochemical reaction [66]. Furthermore, ad-atom deposition growth patterns specificity (determined by the ad-atoms/substrate bonding) can be studied for a particular crystal facet [76]. Therefore, in addition to solving the puzzle of the formic acid electro-oxidation mechanism, research work to tailor the surface of electrocatalyst to improve electrocatalytic activity and selectivity (force the electro-oxidation via direct pathway) is in progress [66].

1.5.1 Surface modification approaches by ad-atoms

There are two approaches to modify the surface of an electrocatalyst. These are “Underpotential deposition” (UPD) and “Irreversible adsorption of ad-atoms” [66]. UPD and dissolution can be presented by the equations 1.14 and 1.15.



$$E_{eq} = E^0 + \frac{RT}{nF} \ln \frac{a^{M^{n+}}}{a^M} \quad (1.15)$$

where “ E_{eq} ” is the equilibrium potential (V), “ E^0 ” the standard potential (V), “ a ” the activity, “ n ” the number of electrons involved in the reaction, “ T ” the temperature (K), “ R ” the gas constant ($J \text{ mol}^{-1} \text{ K}^{-1}$), and “ F ” the Faraday constant ($C \text{ mol}^{-1}$) [77]. The ad-atoms deposited over the surface of the electrocatalyst are oxidized at much more positive potential relative to the potential calculated by the Nernst equation, hence it is called “UPD” as well as metal adsorption, ad-atom deposition, chemisorption of metals, electrodeposition of metals or metal ions, specific adsorption or adsorption of cations or formation of monolayer films [78]. The anomaly of the potential being positive relative to reversible

potential in the electrolyte is due to the stronger bonding interaction between the atoms in bulk solution and substrate, than it is between the atoms in the bulk metal. By manipulating the potential, one can tailor the surface accordingly, however impurities in the bulk solution, metal concentration in the bulk solution and dissolution (potential dependent) may have unfavorable consequences for the overall surface modification via UPD [66].

Irreversible adsorption is a method by which we can modify the electrocatalysts surface by simply dipping an electrode in a solution of precursor metal salt. The metal atoms can be adsorbed on the surface irreversibly such that the adsorbed ad-atoms are stable over a wide range of potential [66, 79, 80]. In UPD, the coverage of the electrocatalyst surface is determined in the presence of the precursor ion (metal salt solution), hence uncertainty can not be ruled out. In the irreversible adsorption method, the electrode is tested in a test solution after modification. The electrocatalytic properties and surface coverage by ad-atoms can be determined precisely in a test solution in the absence of precursor metal solution [81]. Furthermore, the surface coverage by ad-atoms can be controlled by deposition time and concentration of metal solution [66]. The investigation of certain facets of a crystal (particular surface sites) at which the ad-atoms undergo a surface reaction in the absence of a contribution from other surface sites can be investigated [80]. Furthermore, the surface composition of ad-atoms can be altered by manipulating the potential (surface ad-atoms undergo a redox reaction at a certain potential value) [82].

1.5.2 Theoretical justification of ad-atoms modification for catalysis

The electro-oxidation of formic acid is a surface structure dependent reaction [83]. There is an intrinsic limitation to the electro-oxidation of formic acid as it is dependent on

a particular arrangement of surface active sites (ensemble effect). The surface coverage by CO formed by dehydration of formic acid has been found to be only 70%. On the other hand, the surface of an electrode can be covered by CO if it is exposed to CO (gas) [84]. Moreover, the dehydrogenation pathway is also surface structure dependent as Pt(100) has been found to be most electroactive while Pt(111) is the most poison resistant but electroactivity is relatively low [83]. Furthermore, the number of surface active sites required for the dehydrogenation pathway is less relative to the dehydration pathway. Hence surface modification of an electrocatalyst can be used as a tool to increase the selectivity towards the dehydrogenation pathway relative to dehydration pathway [84]. Ad-atoms on the surface of an electrocatalyst as surface modifiers can have three different mechanisms [66]. These are known as “change in the electronic properties of the substrate or electronic effect”, “the third body effect or ensemble effect”, [85] and “the bifunctional effect”[84, 86].

It has been demonstrated that the dehydration pathway requires more adjacent active sites relative to the dehydrogenation pathway. The third body effect is used to disrupt the adjacency among the active sites to force the electro-oxidation via the dehydrogenation pathway [61]. In the third body effect, the ad-atoms are randomly adsorbed over the surface of an electrocatalyst to disrupt the adjacency among active sites while leaving enough active sites required for the dehydrogenation pathway. Cyclic voltametric investigations have revealed that there is an increase in the current (attributed to direct pathway) with an increase in the surface coverage by ad-atoms to a certain limit and then it starts decreasing as the coverage by ad-atoms passes the optimum limit necessary for the direct pathway

[85]. Irreversible adsorption of ad-atoms such as Bi, Sb, Te, Pb, and As has been widely applied to modify Pt single crystal electrodes. These atoms have been found to be effective to disrupt the adjacent Pt active sites (ensembles) necessary for the indirect pathway of formic acid electro-oxidation and thus diminish the indirect oxidation route [87]. Pb on polycrystalline Pt, Bi on Pt(111), and Sb on Pt(100) have been found to increase the electro-oxidation rate up to a factor of 70, 40, and 30, respectively [88]. Formic acid direct oxidation current enhancements of about three times relative to pure Pt have been achieved by use of V group metals to modify the surface as ad-atoms. However, there is no agreement for the optimum coverage of ad-atoms for a particular set of metals and this probably is due to surface structure of different Pt sites, ad-atoms and modification methods employed [61].

The manipulation of electronic properties by surface modification of an electrocatalyst is known as the “electronic effect”. The binding and adsorption energies of the reactants and intermediates depend upon the electronic properties of the surface of an electrocatalyst [66] which is governed by the surface chemical composition and geometric structure [89]. Bimetallic surfaces have different bond lengths than the parent metal and this causes a strain effect that modifies the electronic properties via a change in orbital overlap [90, 91]. Moreover, the interactions between the substrate and ad-atoms change the electronic environment (ligand effect) [86].

In the bifunctional mechanism or bifunctional catalytic effect, the second metal adsorbed at the surface of an electrocatalyst activates water at lower potentials than Pt. The adsorbed ad-atoms facilitate the adsorption of OH (activated water) that can oxidize the adsorbed CO. The removal of CO helps to recover the Pt active sites available for the

electro-oxidation of formic acid via the direct pathway. In other words, the bifunctional catalytic effect is a tool to clean up the poisoned Pt (adsorbed CO) active sites at low potential relative to pure Pt [86, 92].

1.5.3 Pt based surface modified catalysts

Significant enhancement of the oxidation current and a negative shift of the peak potential for formic acid oxidation have been demonstrated by making use of the “third body effect” or “ensemble effect” [62], “bifunctional effect” [79, 85], and/or “electronic effect” of ad-atoms irreversibly adsorbed over the surface of Pt catalysts [61, 85]. Metals such as Ru, Sn, Rh and Au have been used as ad-atoms to improve Pt electroactivity [93]. In addition to the above mentioned metals, ad-atoms such as Se, Cd, Hg, In, Sn, Tl, Bi, Sb and As adsorbed over Pt electrodes have also been studied to improve electroactivity of electrocatalysts towards the electro-oxidation of CO, formic acid, and methanol [94]. Pt(111) surfaces modified by Bi, As, Te, or Sb have been shown to possess high electroactivity relative to the unmodified surface. It has been demonstrated that a very low coverage of ad-atoms has been able to block poisoning via an electronic effect. Ad-atom such as Se showed only a third body effect and the complete blockage of CO formation (poisoning) was achieved only at the maximum coverage [85]. The improvement of electroactivity of Pt modified by Pb ad-atom has been attributed to an electronic effect, while for Pt–Bi catalysts it has been attributed to an electronic effect, third body effect, and a bifunctional mechanism [88]. Among the above mentioned metals atoms of group V used to modify the surface of Pt to improve its electroactivity, Sb has been the most investigated.

Sb has proved to effectively to enhance electroactivity by facilitating the direct pathway via a “third-body” or “electronic effect” [95].

As mentioned above, different ad-atoms improve the electroactivity of Pt via different mechanisms and catalyst surface modification depends upon the nature of the surface and method of modification. Further investigations are necessary to find a catalyst applicable for practical applications in fuel cells.

1.6 Polymer supports for DFAFC catalysts

Supports are used to provide a large surface area, porosity, electrical conductivity and electrochemical stability. All these features are conducive to improving the electroactivity of an electrocatalyst [14]. Conducting polymers (CPs) have technological importance because of their electrical, electronic, magnetic and optical properties. Chemical and physical properties of polymers may be tailored for particular applications. For example, the properties of conjugated polymers can be modulated via doping. Conjugated polymers and metals (gold, silver) have been used to prepare nanomaterials (nanotubes, nanowires, nanoparticles) that can be used for biosensors, catalysis, microelectronics, single electron transistors and nanotips [96]. The electroactivity of catalysts can be enhanced towards the oxidation of organic molecules by making use of CPs as support materials. The enhancement of electroactivity is probably due to their high surface area and/or the synergistic effect between CPs and catalysts such as electronic effects, bifunctional mechanism, electron transport and dispersion of the catalyst [97]. The support effects of CPs for Pt nanoparticles have been focused on polyaniline (PANI), polypyrrole (PPy), polythiophene, polyindole and its derivatives (PIs). Polyaniline and

polyindoles [98], and polycarbazole have been compared [99]. To the best of our knowledge, up to now, there have been no reports on using CPs as the support for Pt nanoparticles along with irreversibly adsorbed metals (Bi,Sb) for the development of catalysts in DFAFC.

1.7 Research objectives

The problem of catalysis is of paramount importance for the oxidation of formic acid as poisoning of Pt blunts electroactivity. It is also known that modification of Pt with oxophilic metals affects dramatically the electrocatalytic behaviour, particularly Bi and Sb. But, the role of Bi and Sb in the changes of catalytic behaviour is not yet really understood. The aim of the present project is to study the activity and selectivity of Pt NP (nanocatalysts) modified by either Bi ad-atoms or Sb ad-atoms toward formic acid electrooxidation. Moreover, the parameters such as deposition time for irreversible adsorption of Bi and Sb ad-atoms over Pt NP have been evaluated along with potential values to avoid the desorption of irreversibly adsorbed ad-atoms. The improvement in the electroactivity of Pt NP catalyst in the presence of adsorbed ad-atoms (Bi, Sb) has been discussed with reference to the literature. Furthermore, the synergic effect of Bi and Sb ad-atoms has been evaluated by adsorption of both (Bi, Sb) on Pt NP. The support effect of polyaniline for Pt NP electroactivity as well as in conjunction with ad-atoms has also been evaluated.

1.8 References

- [1] L. Carrette, K. Friedrich and U. Stimming. Fuel cells—fundamentals and applications. *Fuel Cells 1*, pp. 5-39, 2001.
- [2] A. Appleby. From Sir William Grove to today: Fuel cells and the future. *J. Power Sources 29*, pp. 3-11, 1990.
- [3] J. Andújar and F. Segura. Fuel cells: History and updating. A walk along two centuries. *Renewable and Sustainable Energy Reviews 13*, pp. 2309-2322, 2009.
- [4] E. Ortiz-Rivera, A. L. Reyes-Hernandez and R. A. Febo. Understanding the history of fuel cells. Presented at IEEE Conference on the history of electric power, pp. 117 - 122, 2007.
- [5] A. Kirubakaran, S. Jain and R. Nema. A review on fuel cell technologies and power electronic interface. *Renewable and Sustainable Energy Reviews 13*, pp. 2430-2440, 2009.
- [6] R. M. Ormerod. Solid oxide fuel cells. *Chem. Soc. Rev. 32*, pp. 17-28, 2003.
- [7] L. Carrette, K. A. Friedrich and U. Stimming. Fuel cells: Principles, types, fuels, and applications. *ChemPhysChem 1*, pp. 162-193, 2000.
- [8] B. Frano. PEM fuel cells: Theory and practice, Elsevier Academic Press, New York, 2005.

- [9] K. Sasaki, S. Taniguchi, Y. Shiratori, A. Hayashi, T. Oshima, M. Nishihara, Y. Tachikawa, T. Daio, T. Kawabata and M. Fujita. Smart fuel cell demonstration project: A challenge to realize SOFC-powered campus. *ECS Transactions* 68, pp. 171-178, 2015.
- [10] E. Kjeang, S. Holdcroft, S. Knights, K. Malek, N. Djilali, M. Eikerling, F. Golnaraghi, G. Wang, N. Rajapakse and P. Wild. Development of next generation heavy duty bus fuel cells with enhanced durability. Presented at ECS Meeting Abstracts, 2014.
- [11] B. Han, C. E. Carlton, A. Kongkanand, R. S. Kukreja, B. R. Theobald, L. Gan, R. O'Malley, P. Strasser, F. T. Wagner and Y. Shao-Horn. Record activity and stability of dealloyed bimetallic catalysts for proton exchange membrane fuel cells. *Energy & Environmental Science* 8, pp. 258-266, 2015.
- [12] J. Garche and L. Jürissen. Applications of fuel cell technology: Status and perspectives. *The Electrochemical Society Interface* 24, pp. 39-43, 2015.
- [13] M. Grasemann and G. Laurency. Formic acid as a hydrogen source—recent developments and future trends. *Energy & Environmental Science* 5, pp. 8171-8181, 2012.
- [14] S. Sharma and B. G. Pollet. Support materials for PEMFC and DMFC electrocatalysts—a review. *J. Power Sources* 208, pp. 96-119, 2012.
- [15] G. L. Soloveichik. Liquid fuel cells. *Beilstein Journal of Nanotechnology* 5, pp. 1399-1418, 2014.

- [16] N. V. Rees and R. G. Compton. Sustainable energy: A review of formic acid electrochemical fuel cells. *Journal of Solid State Electrochemistry* 15(10), pp. 2095-2100. 2011.
- [17] D. R. Lycke and S. L. Blair. Fuel cells - exploratory fuel cells -formic acid fuel cells. *Encyclopedia of Electrochemical Power Sources*, pp. 172-181, 2009. DOI: <http://dx.doi.org/10.1016/B978-044452745-5.00864-9>.
- [18] S. Mekhilef, R. Saidur and A. Safari. Comparative study of different fuel cell technologies. *Renewable and Sustainable Energy Reviews* 16, pp. 981-989, 2012.
- [19] M. T. Gencoglu and Z. Ural. Design of a PEM fuel cell system for residential application. *Int J Hydrogen Energy* 34, pp. 5242-5248, 2009.
- [20] X. Zhao, A. Hayashi, Z. Noda, K. Kimijima, I. Yagi and K. Sasaki. Evaluation of change in nanostructure through the heat treatment of carbon materials and their durability for the start/stop operation of polymer electrolyte fuel cells. *Electrochim. Acta* 97, pp. 33-41, 2013.
- [21] N. G. Moreno, M. C. Molina, D. Gervasio and J. F. P. Robles. Approaches to polymer electrolyte membrane fuel cells (PEMFCs) and their cost. *Renewable and Sustainable Energy Reviews* 52, pp. 897-906, 2015.

- [22] Y. Wang, K. S. Chen, J. Mishler, S. C. Cho and X. C. Adroher. A review of polymer electrolyte membrane fuel cells: Technology, applications, and needs on fundamental research. *Appl. Energy* 88, pp. 981-1007, 2011.
- [23] M. K. Debe. Electrocatalyst approaches and challenges for automotive fuel cells. *Nature* 486, pp. 43-51, 2012.
- [24] O. Z. Sharaf and M. F. Orhan. An overview of fuel cell technology: Fundamentals and applications. *Renewable and Sustainable Energy Reviews* 32, pp. 810-853, 2014.
- [25] S. Zhang, X. Yuan, J. N. C. Hin, H. Wang, K. A. Friedrich and M. Schulze. A review of platinum-based catalyst layer degradation in proton exchange membrane fuel cells. *J. Power Sources* 194, pp. 588-600, 2009.
- [26] W. Schmittinger and A. Vahidi. A review of the main parameters influencing long-term performance and durability of PEM fuel cells. *J. Power Sources* 180, pp. 1-14, 2008.
- [27] X. Ou, X. Zhang and S. Chang. Alternative fuel buses currently in use in china: Life-cycle fossil energy use, GHG emissions and policy recommendations. *Energy Policy* 38, pp. 406-418, 2010.
- [28] S. Barrett. FCVs will be a key element in european vehicle powertrains portfolio to achieve 2050 goals. *Fuel Cells Bulletin* 2011, pp. 12-15, 2011.

- [29] K. Haraldsson, A. Folkesson and P. Alvfors. Fuel cell buses in the Stockholm CUTE project—First experiences from a climate perspective. *J. Power Sources* 145, pp. 620-631, 2005.
- [30] Q. Zhigang. *Proton Exchange Membrane Fuel Cells*, CRC Press, 2013.
- [31] S. Renault, S. Gottis, A. Barrès, M. Courty, O. Chauvet, F. Dolhem and P. Poizot. A green Li–organic battery working as a fuel cell in case of emergency. *Energy & Environmental Science* 6, pp. 2124-2133, 2013.
- [32] J. Friedl and U. Stimming. Model catalyst studies on hydrogen and ethanol oxidation for fuel cells. *Electrochim. Acta* 101, pp. 41-58, 2013.
- [33] B. P. Vinayan, R. Nagar, N. Rajalakshmi and S. Ramaprabhu. Novel Platinum–Cobalt alloy nanoparticles dispersed on Nitrogen-Doped graphene as a cathode electrocatalyst for PEMFC applications. *Advanced Functional Materials* 22, pp. 3519-3526, 2012.
- [34] R. B. Moore. Indirect-methanol and direct-methanol fuel cell vehicles. Presented at Energy Conversion Engineering Conference and Exhibit, 2000.(IECEC) 35th Intersociety.
- [35] E. van de Ven, A. Chairuna, G. Merle, S. P. Benito, Z. Borneman and K. Nijmeijer. Ionic liquid doped polybenzimidazole membranes for high temperature proton exchange membrane fuel cell applications. *J. Power Sources* 222, pp. 202-209, 2013.
- [36] W. Zhang, S. Ravi and P. Silva. Application of carbon nanotubes in polymer electrolyte based fuel cells. *Reviews on Advanced Materials Science* 29, pp. 1-14, 2011.

- [37] Y. Gao, C. Tan, L. Ye-Ping, J. Guo and S. Zhang. Formic acid–Formate blended solution: A new fuel system with high oxidation activity. *Int J Hydrogen Energy* 37, pp. 3433-3437, 2012.
- [38] S. Uhm, H. J. Lee and J. Lee. Understanding underlying processes in formic acid fuel cells. *Physical Chemistry Chemical Physics* 11, pp. 9326-9336, 2009.
- [39] S. Z. Rejal, M. S. Masdar and S. K. Kamarudin. A parametric study of the direct formic acid fuel cell (DFAFC) performance and fuel crossover. *Int J Hydrogen Energy* 39, pp. 10267-10274, 2014.
- [40] W. Cai, L. Liang, Y. Zhang, W. Xing and C. Liu. Real contribution of formic acid in direct formic acid fuel cell: Investigation of origin and guiding for micro structure design. *Int J Hydrogen Energy* 38, pp. 212-218, 2013.
- [41] S. K. Kamarudin, W. R. W. Daud, S. L. Ho and U. A. Hasran. Overview on the challenges and developments of micro-direct methanol fuel cells (DMFC). *J. Power Sources* 163, pp. 743-754, 2007.
- [42] M. Broussely and G. Archdale. Li-ion batteries and portable power source prospects for the next 5–10 years. *J. Power Sources* 136, pp. 386-394, 2004.
- [43] Y. Kim, H. J. Kim, Y. S. Kim, S. M. Choi, M. H. Seo and W. B. Kim. Shape-and composition-sensitive activity of pt and PtAu catalysts for formic acid electrooxidation. *The Journal of Physical Chemistry C* 116, pp. 18093-18100, 2012.

- [44] Y. Zhu, S. Y. Ha and R. I. Masel. High power density direct formic acid fuel cells. *J. Power Sources* 130, pp. 8-14, 2004.
- [45] X. Wang, Y. Tang, Y. Gao and T. Lu. Carbon-supported Pd–Ir catalyst as anodic catalyst in direct formic acid fuel cell. *J. Power Sources* 175, pp. 784-788, 2008.
- [46] H. An, H. Cui, D. Zhou, D. Tao, B. Li, J. Zhai and Q. Li. Synthesis and performance of Pd/SnO₂–TiO₂/MWCNT catalysts for direct formic acid fuel cell application. *Electrochim. Acta* 92, pp. 176-182, 2013.
- [47] X. Yu and P. G. Pickup. Recent advances in direct formic acid fuel cells (DFAFC). *J. Power Sources* 182, pp. 124-132, 2008.
- [48] M. Kamarudin, S. Kamarudin, M. Masdar and W. Daud. Review: Direct ethanol fuel cells. *Int J Hydrogen Energy* 38, pp. 9438-9453, 2013.
- [49] C. M. Miesse, W. S. Jung, K. Jeong, J. K. Lee, J. Lee, J. Han, S. P. Yoon, S. W. Nam, T. Lim and S. Hong. Direct formic acid fuel cell portable power system for the operation of a laptop computer. *J. Power Sources* 162, pp. 532-540, 2006.
- [50] S. G. Chalk and J. F. Miller. Key challenges and recent progress in batteries, fuel cells, and hydrogen storage for clean energy systems. *J. Power Sources* 159, pp. 73-80, 2006.
- [51] B. G. Pollet, I. Staffell and J. L. Shang. Current status of hybrid, battery and fuel cell electric vehicles: From electrochemistry to market prospects. *Electrochim. Acta* 84, pp. 235-249, 2012.

- [52] S. Enthaler, J. von Langermann and T. Schmidt. Carbon dioxide and formic acid—the couple for environmental-friendly hydrogen storage? *Energy & Environmental Science* 3, pp. 1207-1217, 2010.
- [53] Y. Pan, R. Zhang and S. L. Blair. Anode poisoning study in direct formic acid fuel cells. *Electrochemical and Solid-State Letters* 12, pp. B23-B26, 2009.
- [54] E. Bertin, S. Garbarino and D. Guay. Formic acid oxidation on Bi covered Pt electrodeposited thin films: Influence of the underlying structure. *Electrochim. Acta* 134, pp. 486-495, 2014.
- [55] G. Samjeské, A. Miki, S. Ye and M. Osawa. Mechanistic study of electrocatalytic oxidation of formic acid at platinum in acidic solution by time-resolved surface-enhanced infrared absorption spectroscopy. *The Journal of Physical Chemistry B* 110, pp. 16559-16566, 2006.
- [56] M. Neurock, M. Janik and A. Wieckowski. A first principles comparison of the mechanism and site requirements for the electrocatalytic oxidation of methanol and formic acid over pt. *Faraday Discuss.* 140, pp. 363-378, 2009.
- [57] W. Gao, J. A. Keith, J. Anton and T. Jacob. Theoretical elucidation of the competitive electro-oxidation mechanisms of formic acid on Pt(111). *J. Am. Chem. Soc.* 132, pp. 18377-18385, 2010.

- [58] J. Xu, D. Yuan, F. Yang, D. Mei, Z. Zhang and Y. Chen. On the mechanism of the direct pathway for formic acid oxidation at a Pt(111) electrode. *Physical Chemistry Chemical Physics* 15, pp. 4367-4376, 2013.
- [59] J. Kim and C. K. Rhee. Ensemble size estimation in formic acid oxidation on Bi-modified Pt (111). *Electrochemistry Communications* 12, pp. 1731-1733, 2010.
- [60] R. B. Moghaddam and P. G. Pickup. Oxidation of formic acid at polycarbazole-supported Pt nanoparticles. *Electrochim. Acta* 97, pp. 326-332, 2013.
- [61] K. Jiang, H. Zhang, S. Zou and W. Cai. Electrocatalysis of formic acid on palladium and platinum surfaces: From fundamental mechanisms to fuel cell applications. *Physical Chemistry Chemical Physics* 16, pp. 20360-20376, 2014.
- [62] F. J. Vidal-Iglesias, A. López-Cudero, J. Solla-Gullón and J. M. Feliu. Towards more active and stable electrocatalysts for formic acid electrooxidation: Antimony-decorated octahedral platinum nanoparticles. *Angewandte Chemie* 125, pp. 998-1001, 2013.
- [63] C. Rice, S. Ha, R. Masel and A. Wieckowski. Catalysts for direct formic acid fuel cells. *J. Power Sources* 115, pp. 229-235, 2003.
- [64] J. Joo, T. Uchida, A. Cuesta, M. T. Koper and M. Osawa. Importance of acid–base equilibrium in electrocatalytic oxidation of formic acid on platinum. *J. Am. Chem. Soc.* 135, pp. 9991-9994, 2013.

- [65] L. Zhang, Z. Wang and D. Xia. Bimetallic PtPb for formic acid electro-oxidation. *J. Alloys Compounds* 426, pp. 268-271, 2006.
- [66] M. T. Koper. *Fuel Cell Catalysis: A Surface Science Approach*, Wiley, 2009.
- [67] V. Grozovski, F. J. Vidal-Iglesias, E. Herrero and J. M. Feliu. Adsorption of formate and its role as intermediate in formic acid oxidation on platinum electrodes. *ChemPhysChem* 12, pp. 1641-1644, 2011.
- [68] A. Cuesta, G. Cabello, M. Osawa and C. Gutiérrez. Mechanism of the electrocatalytic oxidation of formic acid on metals. *Acs Catalysis* 2, pp. 728-738, 2012.
- [69] H. Wang and Z. Liu. Formic acid oxidation at Pt/H₂O interface from periodic DFT calculations integrated with a continuum solvation model. *The Journal of Physical Chemistry C* 113, pp. 17502-17508, 2009.
- [70] J. V. Perales-Rondón, S. Brimaud, J. Solla-Gullón, E. Herrero, R. J. Behm and J. M. Feliu. Further insights into the formic acid oxidation mechanism on platinum: pH and anion adsorption effects. *Electrochim. Acta* 180, pp. 479-485, 2015.
- [71] M. Osawa, K. Komatsu, G. Samjeské, T. Uchida, T. Ikeshoji, A. Cuesta and C. Gutiérrez. The role of Bridge-Bonded adsorbed formate in the electrocatalytic oxidation of formic acid on platinum. *Angewandte Chemie International Edition* 50, pp. 1159-1163, 2011.

- [72] X. Yu and P. G. Pickup. Mechanistic study of the deactivation of carbon supported Pd during formic acid oxidation. *Electrochemistry Communications* 11, pp. 2012-2014, 2009.
- [73] A. Mota-Lima, E. R. Gonzalez and M. Eiswirth. Complex electrooxidation of formic acid on palladium. *Journal of the Brazilian Chemical Society* 25, pp. 1208-1217, 2014.
- [74] F. S. Thomas and R. I. Masel. Formic acid decomposition on palladium-coated Pt (110). *Surf. Sci.* 573, pp. 169-175, 2004.
- [75] N. Hoshi, K. Kida, M. Nakamura, M. Nakada and K. Osada. Structural effects of electrochemical oxidation of formic acid on single crystal electrodes of palladium. *The Journal of Physical Chemistry B* 110, pp. 12480-12484, 2006.
- [76] E. Herrero, L. J. Buller and H. D. Abruna. Underpotential deposition at single crystal surfaces of Au, Pt, Ag and other materials. *Chem. Rev.* 101, pp. 1897-1930, 2001.
- [77] G. Herzog and D. W. Arrigan. Determination of trace metals by underpotential deposition–stripping voltammetry at solid electrodes. *TrAC Trends in Analytical Chemistry* 24, pp. 208-217, 2005.
- [78] S. Szabó. Underpotential deposition of metals on foreign metal substrates. *International Reviews in Physical Chemistry* 10, pp. 207-248, 1991.
- [79] M. C. Figueiredo, A. Santasalo-Aarnio, F. J. Vidal-Iglesias, J. Solla-Gullón, J. M. Feliu, K. Kontturi and T. Kallio. Tailoring properties of platinum supported catalysts by

irreversible adsorbed adatoms toward ethanol oxidation for direct ethanol fuel cells. *Applied Catalysis B: Environmental* 140, pp. 378-385, 2013.

[80] P. Rodríguez, J. Solla-Gullón, F. J. Vidal-Iglesias, E. Herrero, A. Aldaz and J. M. Feliu. Determination of (111) ordered domains on platinum electrodes by irreversible adsorption of bismuth. *Anal. Chem.* 77, pp. 5317-5323, 2005.

[81] Q. Zheng, C. Fan, C. Zhen, Z. Zhou and S. Sun. Irreversible adsorption of Sn adatoms on basal planes of Pt single crystal and its impact on electrooxidation of ethanol. *Electrochim. Acta* 53, pp. 6081-6088, 2008.

[82] M. C. Figueiredo, J. Souza-Garcia, V. Climent and J. M. Feliu. Nitrate reduction on Pt(111) surfaces modified by Bi adatoms. *Electrochemistry Communications* 11, pp. 1760-1763, 2009.

[83] J. Solla-Gullon, F. Vidal-Iglesias, A. Lopez-Cudero, E. Garnier, J. Feliu and A. Aldaz. Shape-dependent electrocatalysis: Methanol and formic acid electrooxidation on preferentially oriented Pt nanoparticles. *Physical Chemistry Chemical Physics* 10(25), pp. 3689-3698, 2008.

[84] W. Vielstich, A. Lamm and H. A. Gasteiger. *Handbook of Fuel Cells: Fundamentals Technology and Applications. Vol. 2*, Wiley, 2003.

[85] A. Boronat-González, E. Herrero and J. Feliu. Fundamental aspects of HCOOH oxidation at platinum single crystal surfaces with basal orientations and modified by

irreversibly adsorbed adatoms. *Journal of Solid State Electrochemistry* 18, pp. 1181-1193, 2014.

[86] F. Vigier, C. Coutanceau, F. Hahn, E. Belgsir and C. Lamy. On the mechanism of ethanol electro-oxidation on Pt and PtSn catalysts: Electrochemical and in situ IR reflectance spectroscopy studies. *J Electroanal Chem* 563, pp. 81-89, 2004.

[87] Q. Chen, Z. Zhou, F. J. Vidal-Iglesias, J. Solla-Gullón, J. M. Feliu and S. Sun. Significantly enhancing catalytic activity of tetrahedral Pt nanocrystals by Bi adatom decoration. *J. Am. Chem. Soc.* 133, pp. 12930-12933, 2011.

[88] M. D. Obradović, A. V. Tripković and S. L. Gojković. The origin of high activity of Pt–Au surfaces in the formic acid oxidation. *Electrochim. Acta* 55, pp. 204-209, 2009.

[89] H. Xin, A. Vojvodic, J. Voss, J. K. Nørskov and F. Abild-Pedersen. Effects of d-band shape on the surface reactivity of transition-metal alloys. *Physical Review B* 89, pp. 115114, 2014.

[90] J. Kitchin, J. K. Nørskov, M. Barteau and J. Chen. Modification of the surface electronic and chemical properties of Pt (111) by subsurface 3d transition metals. *J. Chem. Phys.* 120, pp. 10240-10246, 2004.

[91] T. Bligaard and J. K. Nørskov. Ligand effects in heterogeneous catalysis and electrochemistry. *Electrochim. Acta* 52(18), pp. 5512-5516, 2007.

- [92] G. Li and P. G. Pickup. The promoting effect of Pb on carbon supported Pt and Pt/Ru catalysts for electro-oxidation of ethanol. *Electrochim. Acta* 52, pp. 1033-1037, 2006.
- [93] B. Liu, J. Jin, X. Lin, C. Hardacre, P. Hu, C. Ma and W. Lin. The effects of stepped sites and ruthenium adatom decoration on methanol dehydrogenation over platinum-based catalyst surfaces. *Catalysis Today* 242, pp. 230-239, 2015.
- [94] V. Tripkovic. First principles study of (Cd, Hg, In, Tl, Sn, Pb, As, Sb, Bi, Se) modified Pt (111), Pt (100) and Pt (211) electrodes as CO oxidation catalysts. *Electrochim. Acta* 168, pp. 370-378, 2015.
- [95] B. Peng, J. Wang, H. Zhang, Y. Lin and W. Cai. A versatile electroless approach to controlled modification of Sb on Pt surfaces towards efficient electrocatalysis of formic acid. *Electrochemistry Communications* 11, pp. 831-833, 2009.
- [96] T. Ahuja and D. Kumar. Recent progress in the development of nano-structured conducting polymers/nanocomposites for sensor applications. *Sensors Actuators B: Chem.* 136, pp. 275-286, 2009.
- [97] R. B. Moghaddam, O. Y. Ali, M. Javashi, P. L. Warburton and P. G. Pickup. The effects of conducting polymers on formic acid oxidation at Pt nanoparticles. *Electrochim. Acta*, pp. 230-236, 2014.

[98] W. Zhou, Y. Du, H. Zhang, J. Xu and P. Yang. High efficient electrocatalytic oxidation of formic acid on Pt/polyindoles composite catalysts. *Electrochim. Acta* 55, pp. 2911-2917, 2010.

[99] R. B. Moghaddam and P. G. Pickup. Influences of aniline, carbazole, indole, and pyrrole monomers and polymers on formic acid oxidation at Pt electrodes. *Electrochim. Acta* 107, pp. 225-230, 2013.

CHAPTER 2

Experimental

2 Experimental

2.1 Chemicals

All chemicals were used as received. Sulphuric acid (Fisher Scientific), $\text{H}_2\text{PtCl}_6 \cdot 6\text{H}_2\text{O}$ (Alfa Aesar), sodium citrate (Anachemia), formic acid (Sigma Aldrich; 98-100%), sodium borohydride (Sigma-Aldrich), Sb(III) oxide (Sigma Aldrich). Doubly distilled water having a resistivity of $18.0 \Omega \cdot \text{m}$ was used for the experiments.

2.2 Synthesis of Pt nanoparticles (NP)

Pt NP were prepared by mixing and stirring an aqueous solutions of $\text{H}_2\text{PtCl}_6 \cdot 6\text{H}_2\text{O}$ (10 mL; 3.00 mM) and sodium citrate (0.60 mL; 50 mM) followed by drop wise addition of aqueous NaBH_4 (160 mM; 0.8 mL) with continuous stirring for further two hours. The resulting Pt NP colloidal solution was stored in a fridge. Previously, this procedure has been found to consistently produce nanoparticles with an average diameter of ca. 5 nm [1]. Active areas, determined electrochemically, were consistent with this average size.

2.3 Preparation of working electrodes

Glassy carbon electrodes (GC; CH Instruments; 0.071 cm^2) were polished with $0.05 \mu\text{m}$ alumina, washed with distilled water, and sonicated for 10 min before use. The GC electrodes were drop coated with Pt NP ($1.25 \mu\text{L}$), dried in air and washed with $0.1 \text{ M H}_2\text{SO}_4$ before voltammetric experiments. The solution immersion method was used to adsorb ad-atoms onto the Pt NP [2]. Ad-atoms were adsorbed by immersing the GC/Pt electrode in a solution of $0.1 \text{ mM Sb}_2\text{O}_3$ or $0.1 \text{ mM Bi}_2\text{O}_3$ in $0.1 \text{ M H}_2\text{SO}_4$ or $0.5 \text{ M H}_2\text{SO}_4$ at open circuit. The molarity of the metal solution was varied for evaluation of the optimum

concentration for irreversible adsorption. The amount of adsorption/coverage was controlled by varying the immersion time. The electrodes were rinsed with double distilled water and introduced into a cell containing 0.1 M H₂SO₄ supporting electrolyte for cyclic voltammetric and chronoamperometric experiments.

Polyaniline (PANI) as a support was prepared by galvanostatic polymerization. Aniline (0.1 M) in 0.5 M H₂SO₄ was introduced into a three electrode (Pt wire, GC electrode, SCE) glass cell and it was subjected to galvanostatic polymerization (I=3.5 μA, t=150 s) [1]. The GC electrode coated with PANI was washed with distilled water and it was drop coated with Pt NP.

2.4 Instrumentation

A Pine Instrument Company potentiostat (RDE4) coupled with customized data acquisition software was used to perform cyclic voltammetry (CV) and chronoamperometry (CA) experiments. Electrochemistry experiments were performed by using a three electrode glass cell. A saturated calomel electrode (SCE) was used as the reference electrode and Pt wire as the counter electrode. Sulphuric acid (0.1 M) was used as the supporting electrolyte.

2.5 Voltammetric experiments

The GC/Pt NP electrodes were characterized by using cyclic voltammetry. The current was measured from -250 mV to 800 mV vs. SCE at a scan rate of 100 mVs⁻¹. This scan rate was used for all background voltammograms unless otherwise stated. The test solution (0.1 M H₂SO₄) was deaerated with nitrogen gas for 15 min before each experiment

and nitrogen flow was maintained over the solution to avoid environmental air exchange. Formic acid oxidation experiments were conducted at a scan rate of 10 mVs^{-1} . A potential window of -250 mV to 400 mV vs. SCE was used for the Sb modified GC/Pt NP experiments. The upper limit of the potential sweep (400 mV) was chosen to maintain the stability of Sb ad-atoms adsorbed at Pt. In the case of Bi modified Pt NP experiments, the positive potential was varied and it is given in the experimental data discussed in the results and discussion section. For Sb and Bi modified Pt NP experiments, nitrogen was continuously bubbled through the test solution.

2.6 References

- [1] R. B. Moghaddam and P. G. Pickup. Support effects on the oxidation of ethanol at Pt nanoparticles. *Electrochim. Acta* 65, pp. 210-215, 2012.
- [2] F. J. Vidal-Iglesias, A. López-Cudero, J. Solla-Gullón and J. M. Feliu. Towards more active and stable electrocatalysts for formic acid electrooxidation: Antimony-Decorated octahedral platinum nanoparticles. *Angewandte Chemie* 125, pp. 998-1001, 2013.

CHAPTER 3

Sb ad-atoms and their enhancement effects on Pt activity for formic acid oxidation

3 Sb ad-atoms and their enhancement effects on Pt activity for formic acid oxidation

3.1 Introduction

The electro-oxidation of formic acid on Pt is considered as a model reaction to understand and interpret the rudimentary aspects of electrocatalytic reactions. The reason for the selection of formic acid as a model reaction is that only two electrons are involved. The C-C bond cleavage is not involved as in the case of ethanol. Pt is very active towards dehydrogenation processes. However, Pt is susceptible to poisoning because of formation of adsorbed CO via dehydration of formic acid [1, 2].

The dehydrogenation reaction, as well as the poisoning of Pt by adsorbed CO via dehydration of formic acid, is highly sensitive to the surface structure of the catalyst [1, 3]. The dehydration reaction is site specific and modification of the surface by blocking sites can improve the electrocatalytic activity of Pt [1].

Ad-atoms such as Sb, Pd, Ru, Se, Bi, Pb and As have been used to block surface sites and improve the electroactivity of Pt by third body and/or electronic effects [4]. Sb has been used as an ad-atom via solution deposition as well as via underpotential deposition onto Pt to modify the surface properties and inhibit the adsorption of CO via the dehydration reaction [2, 4, 5]. The Sb ad-atoms on Pt have been shown to block poisoning of Pt (adsorption of CO) by a third body effect at a

variety of Pt surfaces such as polycrystalline Pt, Pt(100), Pt(320), Pt(331) and Pt(110) [1-5].

This chapter reports the relationships between Sb coverage, immersion time (GC/Pt electrode immersed in Sb solution) and electroactivity for formic acid oxidation at Sb ad-atom modified Pt. The long term activity of the Sb modified Pt as well as the maximum achievable coverage is reported.

3.2 Results and Discussion

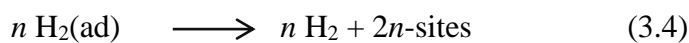
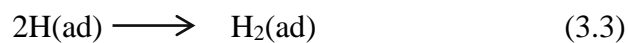
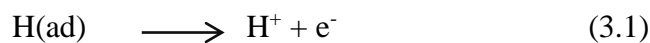
3.2.1 Determination of surface area of the platinum nanoparticles (Pt NP)

In electrochemistry, the “real surface area” is the area of the electrode or catalyst that determines the electroactivity. There can be a large difference between the real surface area (active area) and the geometric surface area of the electrode [6-8]. There are various methods used to determine the real or active surface area of an electrocatalyst such as capacitance ratio, oxygen adsorption from solution, drop weight (or volume), and hydrogen adsorption [8, 9].

Hydrogen underpotential adsorption/desorption (HUPD) is one of the simplest and fastest electrochemical processes [10]. The HUPD voltammetric profile depends on the solution, scan rate, and potential sweep window [8]. Also, the HUPD processes are highly dependent on the surface lattice structure [8, 11]. For example, Pt(100) and Pt(110) give only one predominant peak in voltammograms, while Pt(111) shows no clear peaks [10, 12]. The surface area of the GC/Pt (Pt NP) electrodes used here have been determined by using the hydrogen desorption method. There are two assumptions for this method: “the potential at which the hydrogen forms a monolayer at the surface of the electrocatalyst is at the onset of the hydrogen evolution and the relation between adsorbed hydrogen and platinum atoms is one to one” [8, 9].

Before performing formic acid oxidation experiments, Pt NP were examined by CV to establish the surface area of the Pt NP and their stability. Figure 3.1 shows a voltammogram of GC/Pt (GC electrode coated with 0.64 μg of Pt NP) in 0.1 M

H₂SO₄ at a scan rate of 100 mV s⁻¹. A second scan was taken for the surface area measurement. The reason to take the second scan is to activate the electrode by the irreversible oxidation of adsorbed organic impurities on the electrode surface during the 1st scan [7]. This is the reason that the first scan (not shown) is different from the subsequent scans. Three regions can be distinguished in the voltammogram presented in Fig 3.1. The shaded anodic area (blue) at low potentials represents the hydrogen desorption region followed by low currents (negative (cathodic) for the negative sweep and positive (anodic) for the positive sweep) representing the double layer region where only capacitive processes take place. The shaded cathodic area (red) represents the hydrogen adsorption region at negative potentials [7]. The hydrogen evolution, hydrogen adsorption and desorption can be depicted by equations 3.1 to 3.4.



The charge associated with the formation of a monolayer of H atoms (Q) can be calculated by integration of the adsorption or desorption peaks or taking an average of the integrated area of both peaks as shown by equations 3.5 and 3.6 [7].

$$Q = 1/v \int_{(V_0-V_i)/v}^{(V_0-V_f)/v} I dV \quad (3.5)$$

$$Q = 1/v \int_{(V_0-V_i)/v}^{(V_0-V_f)/v} I dV - Q_{dl} \quad (3.6)$$

The V_0 and v represent the initial potential and potential sweep rate while V_i and V_f are the potentials at the start of hydrogen adsorption and at the completion of monolayer formation, respectively. Equation (3.6) represents the subtraction of the capacitance charge Q_{dl} as the capacitive current is not restricted to the capacitive region. It extends over the whole range of electrode potentials and it is present over all regions of the voltammogram [7, 13]. The charge calculated by using equation (3.6) corresponds to the surface area of the catalyst that is based on crystal structure. For polycrystalline Pt NP, the accepted conversion factor is $210 \mu\text{C cm}^{-2}$ [9, 14]. By using equation (3.6) and dividing the obtained value by $210 \mu\text{C cm}^{-2}$, the final calculated value was 0.23 cm^2 or $37.17 \text{ m}^2 \text{ g}^{-1}$ for the Pt NP used here. The formation of platinum oxide above 550 mV and HUPD peaks appearing below 100 mV confirm the high purity of Pt (Pt NP). Oxide formation solely depends on the potential. The onset of oxide formation starts with interaction of water molecules with the electrocatalyst surface and, consequently, the formation of an adsorbed layer of oxide or hydroxide containing species on the electrode surface. The persistent increase in the current density of the oxidation region (550-1000 mV) is attributed to the formation of surface oxide [15].

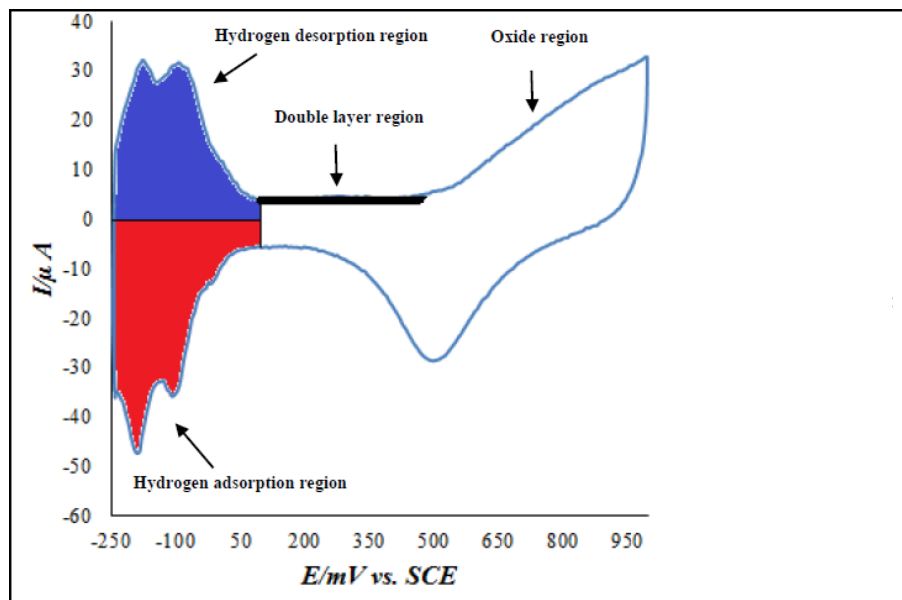


Figure 3.1. Cyclic voltammogram (100 mV s^{-1}) of a GC/Pt electrode (Pt NP = $0.64 \mu\text{g}$) in $0.1 \text{ M H}_2\text{SO}_4$

The appearance of well-defined oxidation and reduction peaks of the platinum are typical of a clean platinum surface [14]. The hydrogen desorption (blue part in the Fig 3.1) was integrated to eliminate the charge contribution of the GC background and hydrogen evolution.

3.2.2 Oxidation of formic acid

The oxidation of formic acid on GC / Pt (Pt NP) is illustrated by the CV in the Fig 3.2. The mechanism of formic acid electro-oxidation has two different pathways. Oxidation occurs through an active intermediate (formate ion/direct pathway/dehydrogenation) or via a poisoning intermediate (indirect pathway/dehydration), CO, adsorbed at the surface of the electrocatalyst [16-18]. The two pathways of the formic acid oxidation can be identified in the voltammogram

shown in Fig 3.2. On the anodic scan, there are two peaks. The 1st peak and 2nd peak represent the direct and indirect pathways, respectively. On the anodic scan, the current began to increase at a potential of about 10 mV and the onset of the second peak was at ca. 440 mV. The current was very low for the 1st peak in the positive going scan because carbon monoxide (CO) had blocked the surface of the electrocatalyst and formate ion could not access the electrocatalyst active sites [1].

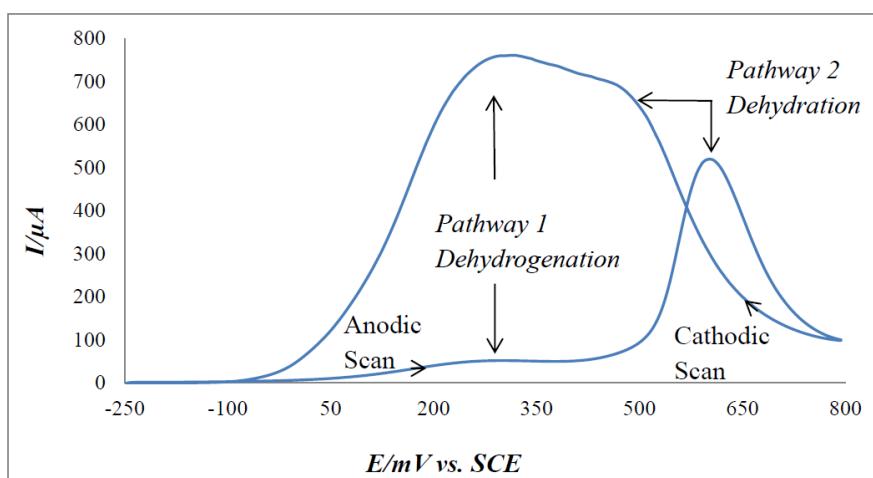


Figure 3.2. Voltammogram (10 mV s^{-1}) of GC/Pt (Pt NP = $0.64 \mu\text{g}$) electrode in $0.1 \text{ M H}_2\text{SO}_4 + 0.5 \text{ M HCOOH}$.

The blockage of the electrocatalyst surface by CO can't be removed unless water molecules are activated at higher potentials to give hydroxyl ions adsorbed at sites nearby the adsorbed CO. This is the reason that on pure Pt, electro-oxidation of formic acid proceeds via the 2nd or indirect pathway, predominantly. As the potential reached the value for the oxidation of Pt, adsorbed OH is readily available to oxidize adsorbed CO and the current increased by almost 10 times relative to the 1st anodic

peak. On the cathodic sweep, there are also two processes. The mechanism of the shoulder at ca. 950 mV is exactly the same as the 2nd peak of the anodic sweep. The difference is that the oxidation of CO is taking place at a freshly reduced electrocatalyst surface. The peak in the cathodic sweep at ca. 300 mV gave a very high current compared to its corresponding peak (pathway 1) in the anodic scan (formate ion/direct pathway) because it is happening at the freshly reduced, poison free (CO free) surface of the electrocatalyst. The peak currents are highly dependent on the potential applied and it proves that the formic acid electro-oxidation reaction is highly dependent on the chemistry and the structure of the electrocatalyst [1, 17, 19, 20].

3.2.3 Oxide formation and stability of Sb ad-atoms

Fig 3.3 presents cyclic voltammograms of a GC/Pt-Sb electrode. There is a redox couple at ca. 450 mV that can be attributed to oxidation/reduction of the adsorbed ad-layer of Sb on the polycrystalline Pt NP [21]. The oxidation peak appears at ca. 450 mV and shifts towards positive potential with each scan. This is probably due to the loss of Sb ad-atoms by each scan. As the coverage is lost gradually with each scan, the current due to oxidation decreases and it has decreased noticeably in the 3rd scan compared to the 1st scan.

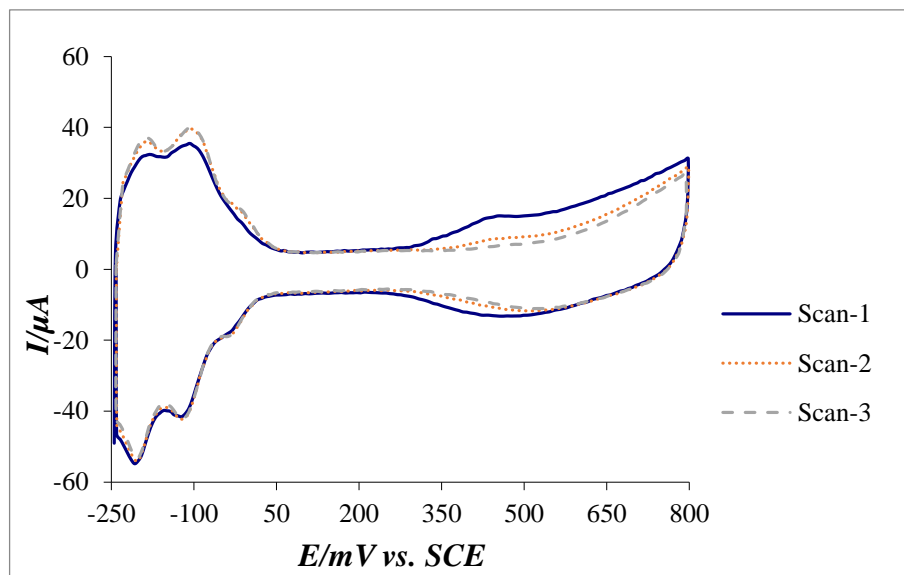
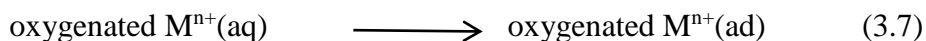


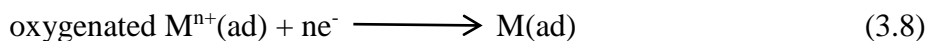
Figure 3.3. Voltammograms (100 mV s^{-1}) of GC/Pt (Pt NP = $0.64 \mu\text{g}$) electrodes that had been immersed in $0.1 \text{ mM Sb}_2\text{O}_3 + 0.1\text{M H}_2\text{SO}_4$ for 1 min.

The stability of irreversibly adsorbed Sb and its dependency on the applied potential could be explained by understanding the irreversible adsorption process of Sb at Pt. The adsorption process involves the adsorption of oxygenated (oxy or hydroxyl metal complexes) metal cations onto the electrode surface [22]. The irreversible adsorption takes place between the electrode to be modified and a solution of metal oxide in dilute acid. The overall process of adsorption can be depicted by equations 3.7 to 3.10 [22].

Adsorption (SbO_{ad} , $[\text{SbOH}]_{\text{ad}}$)



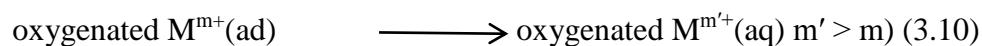
Electrochemical reduction to elemental metal atoms



Electrochemical oxidation



Stripping of the adsorbed oxygenated metal atoms



At fairly positive open circuit potentials, metal cations associated with oxide or hydroxide anions in aqueous solution form positively charged oxy metal ions being adsorbed at the electrode surface. These adsorbed oxygenated ad-atoms of the metal undergo electrochemical reduction to be converted to neutral metal atoms. The adsorbed elemental ad-atoms can be oxidized and stripped off according to equations 3.9 and 3.10. The potential needed to strip off ad-atoms is higher than the potential at which oxygenated metal species adsorb on the electrode [22].

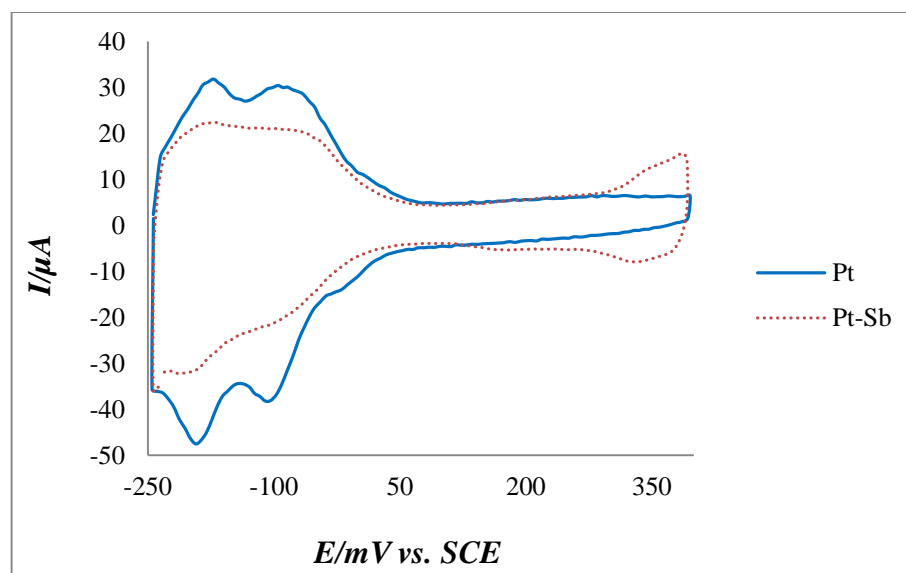


Figure 3.4. Voltammograms (100 mV s^{-1}) of GC/Pt (Pt NP = $0.64 \mu\text{g}$) and GC/Pt electrodes modified by immersion in $0.1 \text{ mM Sb}_2\text{O}_3 + 0.1 \text{ M H}_2\text{SO}_4$ for 30 min.

Fig 3.4 presents voltammograms of Pt modified with Sb and unmodified Pt in 0.1 M H₂SO₄. Only HUPD peaks are observed at potentials lower than ca. 250 mV and this indicates the stability of the adsorbed ad-atoms of Sb on Pt at potentials lower than ca. 250 mV. The oxidation of Sb at lower positive potential than Pt (the onset potential of oxidation of Pt is ca. 550 mV (Fig 3.1)) itself shows that the Sb ad-atoms have the ability to adsorb OH at lower potentials than Pt. As the indirect pathway of formic acid oxidation involves oxidation of CO by adsorbed OH, this ability of oxygen adsorption at low potentials by Sb relative to Pt should increase the electroactivity of Sb modified Pt towards formic acid oxidation by the indirect pathway [4].

3.2.4 Dependence of Sb coverage on immersion time

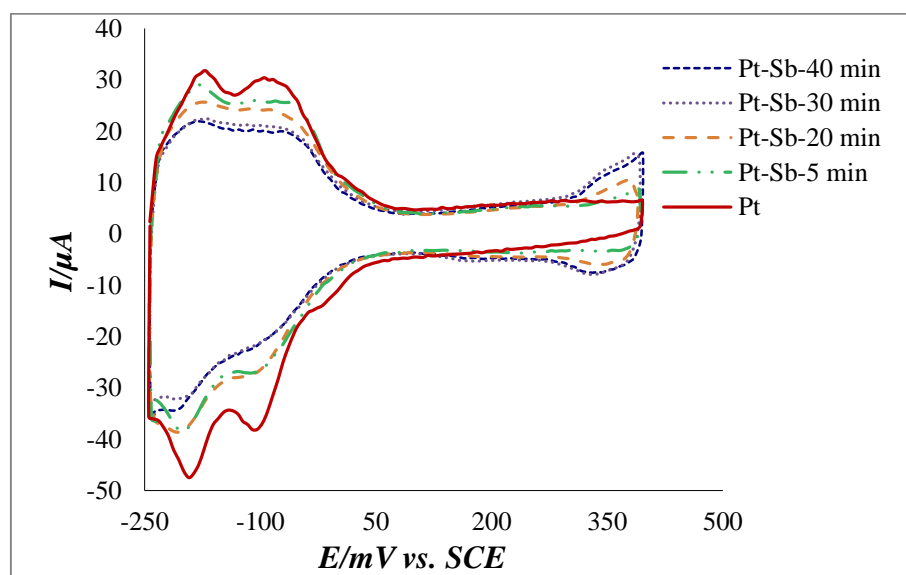


Figure 3.5. Voltammograms (100 mV s^{-1}) of GC/Pt (Pt NP = $0.64 \mu\text{g}$) and GC/Pt electrodes immersed for x min in $0.1 \text{ mM Sb}_2\text{O}_3$ and tested in $0.1 \text{ M H}_2\text{SO}_4$.

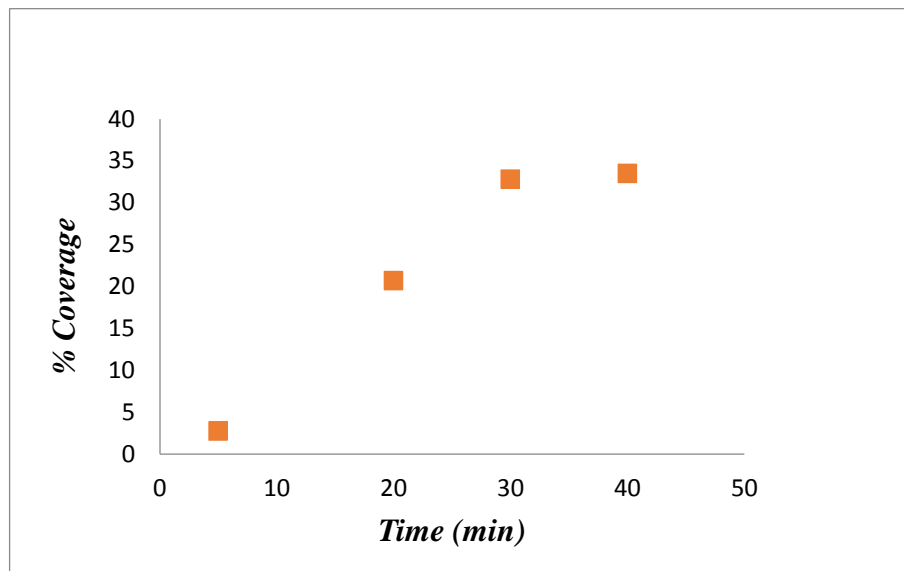


Figure 3.6. Relationship between Sb ad-atom coverage and immersion time.

Fig 3.5 shows voltammograms of Pt and Pt electrodes modified by Sb at different immersion times. The peaks below 50 mV are due to HUPD on the active sites of the polycrystalline Pt. The coverage on the Pt by Sb ad-atoms is dependent on immersion time. This is evident from the HUPD peaks decreasing intensity, sharpness, and reversibility with increasing immersion time [23]. The oxidation peak of Sb at ca. 350 mV is also in accordance with the changing amount of the adsorbed Sb. As the immersion time was increased, the amount of adsorbate increased and the intensity of the oxidation peak increases. The position of the oxidation peak can be used as a guide to set up the potential sweep window. The Sb ad-atoms are stable until 280 mV. This indicates that the ad-atoms are present in elemental form over the platinum active sites and we can produce stable and reversible voltammograms within the positive potential limit of 280 mV.

Fig 3.6 shows the relationship between coverage (%) of ad-atoms and immersion time. Surface area of the Pt NP was calculated by using equation (3.6) given above. The percent coverage was calculated by taking the difference in the charge values under the hydrogen desorption peaks for Pt NP and Pt NP modified by Sb ad-atom (Fig 3.5). The maximum coverage achieved was ca. 33% at an immersion time of 40 min. The percent coverage achieved at immersion times of 30 and 40 min was almost the same. This implies that the optimum immersion time is about 30 min for the maximum achievable coverage of about 33% in 0.1 mM Sb_2O_3 dissolved in 0.1 M H_2SO_4 . A low saturation point could be explained by the limited availability of oxygenated metal cations (only oxy/hydroxyl metal cations can be adsorbed at an electrode surface [22, 24]) under the conditions employed (0.1 M H_2SO_4 , $\text{pH} \approx 1$) [25].

3.2.5 Formic acid oxidation: cyclic voltammetry

Fig 3.7 shows cyclic voltammograms of GC/Pt and GC/Pt-Sb electrodes tested in 0.1 M H_2SO_4 + 0.5 M HCOOH . The purpose of the experiment was to test the role of Sb coverage over Pt in the oxidation of HCOOH .

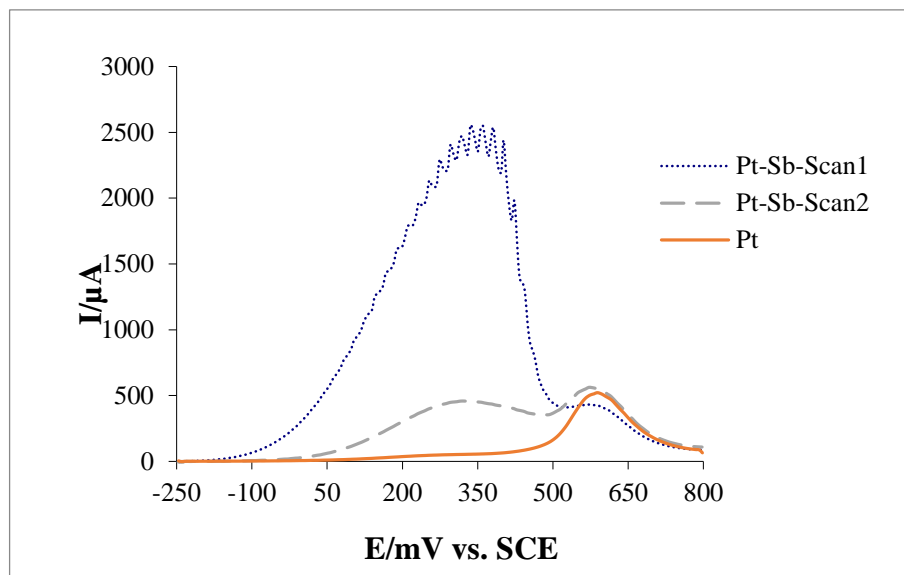


Figure 3.7. Anodic scans (10 mV s^{-1}) of GC/Pt (Pt NP = $0.64 \mu\text{g}$) and GC/Pt electrodes immersed for 30 min in $0.1 \text{ mM Sb}_2\text{O}_3$ and tested in $0.1 \text{ M H}_2\text{SO}_4 + 0.5 \text{ M HCOOH}$.

We can see an increase of almost 50 times in the rate (current) of the direct pathway for oxidation of formic acid relative to the unmodified Pt. At the high oxidation current, there were bubbles at the tip of the electrode because of CO_2 production and the bursting of bubbles gave oscillations in the current for the first scan of the voltammograms (Fig 3.7). The indirect pathway of oxidation of formic acid was slightly suppressed at the GC/Pt-Sb electrode as most of the oxidation occurred through the direct pathway. In other words, the poison formation has been decreased significantly by Sb ad-atoms over the Pt surface. As the oxidation of formic acid depends upon the nature of the surface of the catalyst, the modified surface (Pt-Sb) is much less susceptible to poison formation. The much lower current for the direct pathway in the subsequent scan is due to the loss of Sb ad-atoms by oxidation at the high positive potentials employed.

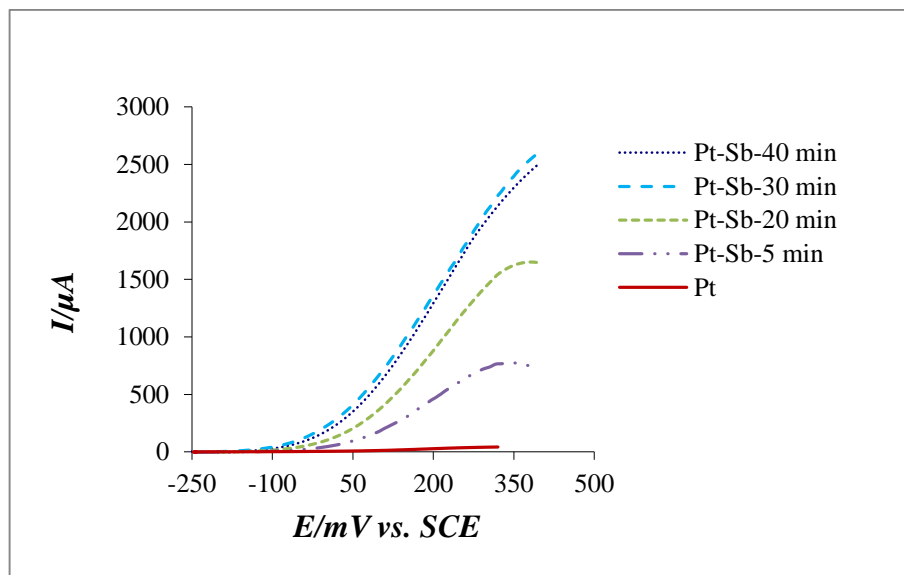


Figure 3.8. Anodic scans (10 mV s^{-1}) of GC/Pt (Pt NP = $0.64 \mu\text{g}$) and GC/Pt electrodes immersed for x min in in $0.1 \text{ mM Sb}_2\text{O}_3$ and tested in $0.1 \text{ M H}_2\text{SO}_4 + 0.5 \text{ M HCOOH}$.

Fig 3.8 shows the effect of deposition time on the electroactivity of the Sb ad-atoms modified Pt for formic acid oxidation. The onset potential for the direct pathway of formic acid oxidation on Pt is much higher than for the Sb ad-atom modified Pt. In addition, there is a significant increase in the peak current and decrease in the onset potential for the direct pathway of oxidation of formic acid with increase in deposition time.

The oxidation at lower potential by Sb modified Pt shows that there is significant improvement in the electroactivity of the catalyst (Sb modified Pt). The enhanced activity by GC/Pt-Sb has been mainly attributed to the third body effect but the change in the onset potential (oxidation at lower potential) indicates that Sb can play the role of a true catalyst [4, 26]. For the route through the direct pathway, the electronic effect of Sb can increase the intrinsic activity of the Pt and hence decrease

the onset potential [1, 2]. However, XPS data suggests it is a third body effect rather than an electronic effect [4].

As seen in Fig 3.5, the onset potential for the oxidation of Sb ad-atoms at Pt is about 300 mV whereas the peak current for the direct pathway of formic acid oxidation at Sb modified Pt is at about 400 mV. Hence, a contribution of Sb ad-atoms towards oxidation of formic acid via the indirect pathway cannot be ruled out. Therefore, the Sb ad-atoms not only have the third body effect but may also have an electrocatalytic effect via the bifunctional mechanism [2].

3.2.6 Dependence of formic acid oxidation activity on Sb coverage

Fig 3.9 shows the relationship between the electroactivity of GC/Pt-Sb and Sb coverage at Pt. It can be seen that a small amount of Sb ad-atoms have a large effect on the activity of Pt by blocking poison formation. The coverage and activity can be correlated directly.

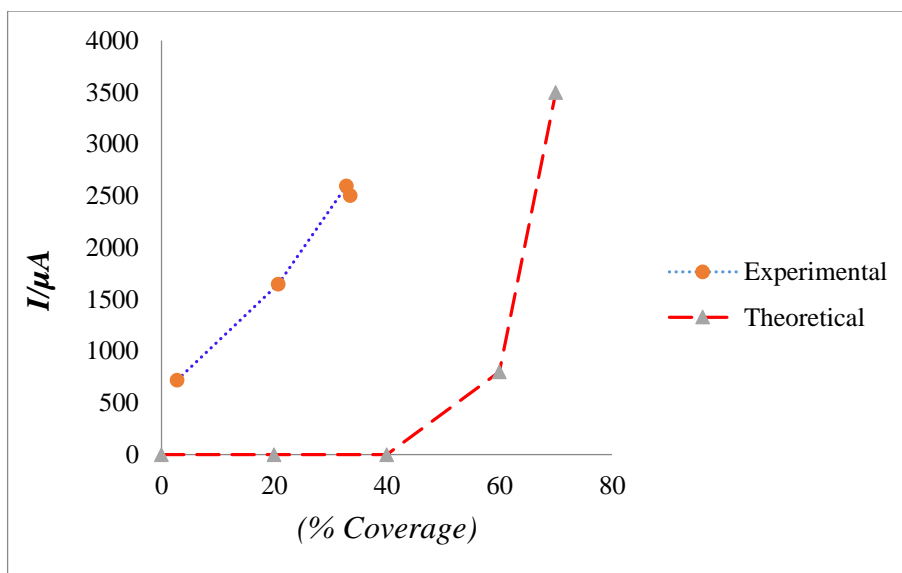


Figure 3.9. Electroactivity for formic acid oxidation at 395 mV versus Sb coverage (%) over Pt (experimental curve) and experimental curve comparison with theoretical model curve (current versus ad-atom coverage curve for the case where the ad-atoms are assumed to be catalytically inert and the current is originated only from those substrate atoms which were protected from poisoning).

A theoretical model was used to mimic the behaviour of Sb randomly deposited for the catalysis of formic acid in sulfuric acid [26]. In that model (theoretical curve in Fig 3.9), Sb was supposed to have only a third body effect and the depicted relationship between coverage (Sb coverage at Pt) and electroactivity for formic acid oxidation was not linear. The experimental curve shown in Fig 3.9

deviates from that model. The deviation can be explained by considering that the Sb has a third body effect as well as electronic and bifunctional effects [5].

3.2.7 Long-term activity test: chronoamperometry

The long term activity of an electrocatalyst is very important for its actual application in a fuel cell. The long term activity can be tested by applying a

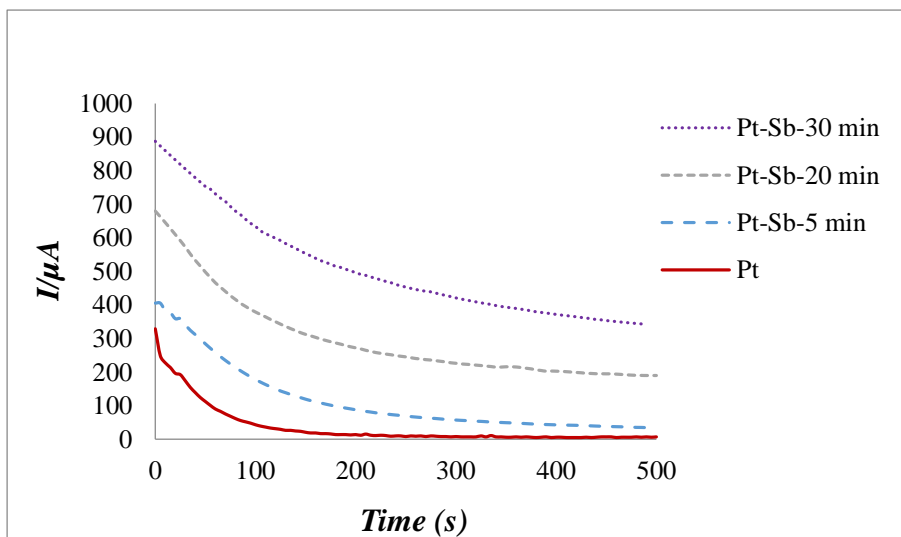


Figure 3.10. Chronoamperometry at 100 mV for GC/Pt (Pt NP = 0.64 μg) and GC/Pt electrodes that has been immersed for x min in 0.1 mM Sb_2O_3 , tested in 0.1 M H_2SO_4 + 0.5 M HCOOH .

constant potential for an extended period of time. The GC/Pt and GC/Pt-Sb electrodes were tested at +0.1 V for a time of 500 s. The results are in accordance with the CV (Fig 3.10) results as the current increased with increasing deposition time. However, at all Sb coverages, current decreased steadily with time. The decrease in the current values at such a low potential (+0.1 V) at which the Sb ad-atoms are stable and should not dissolve, may be attributed to the poisoning of the Pt electrocatalyst by CO. As

we could achieve only 33% coverage by Sb ad-atoms, there is almost 67% of uncovered surface area of the Pt. The uncovered surface area (the area having two consecutive free Pt sites for CO formation) is exposed to CO and its accumulation would result in decreasing current during constant potential chronoamperometry experiments. A second reason for decreasing values of current in constant potential experiments could be the leaching of the adsorbed ad-atoms in the presence of formic acid [27].

3.3 Conclusions

Drop coated Pt (Pt NP) on GC electrodes was modified by Sb via a solution immersion method and shown to produce powerful electrocatalysts for formic acid oxidation. GC/Pt-Sb electrocatalysts have shown an improvement of 50 times in the electroactivity for formic acid oxidation relative to a GC/Pt electrode. There was an improvement in the onset potential of formic acid oxidation too (+100 mV for GC/Pt, -50 mV for GC/Pt-Sb). The maximum achievable coverage of Sb onto Pt was found to be about 33%. The coverage (%) versus electroactivity has been found to be linearly correlated. Long term activity tests at constant potential for the GC/Pt-Sb showed an improved resistance to poisoning (formation of CO) relative to GC/Pt.

3.4 References

- [1] A. Boronat-González, E. Herrero and J. Feliu. Fundamental aspects of HCOOH oxidation at platinum single crystal surfaces with basal orientations and modified by irreversibly adsorbed adatoms. *Journal of Solid State Electrochemistry* 18, pp. 1181-1193, 2014.
- [2] F. J. Vidal-Iglesias, A. López-Cudero, J. Solla-Gullón and J. M. Feliu. Towards more active and stable electrocatalysts for formic acid electrooxidation: Antimony-decorated octahedral platinum nanoparticles. *Angewandte Chemie* 125, pp. 998-1001, 2013.
- [3] Y. Yang, S. Sun, Y. Gu, Z. Zhou and C. Zhen. Surface modification and electrocatalytic properties of Pt (100), Pt (110), Pt (320) and Pt (331) electrodes with Sb towards HCOOH oxidation. *Electrochim. Acta* 46, pp. 4339-4348, 2001.
- [4] J. K. Lee, H. Jeon, S. Uhm and J. Lee. Influence of underpotentially deposited Sb onto Pt anode surface on the performance of direct formic acid fuel cells. *Electrochim. Acta* 53, pp. 6089-6092, 2008.
- [5] Y. Yang, Z. Zhou and S. Sun. In situ FTIRS studies of kinetics of HCOOH oxidation on Pt (110) electrode modified with antimony adatoms. *J Electroanal Chem* 500, pp. 233-240, 2001.
- [6] S. Campbell, J. Smith, G. Lloyd, F. Walsh and T. Ralph. Electrochemical and microscopic characterisation of platinum-coated perfluorosulfonic acid (Nafion 117) materials. *Analyst* 123, pp. 1923-1929, 1998.

- [7] J. M. Doña Rodríguez, J. A. Herrera Melián and J. Pérez Peña. Determination of the real surface area of Pt electrodes by hydrogen adsorption using cyclic voltammetry. *J. Chem. Educ.* 77, pp. 1195, 2000.
- [8] W. Vielstich, A. Lamm and H. A. Gasteiger. *Handbook of Fuel Cells: Fundamentals Technology and Applications. Vol. 2*, Wiley, 2003.
- [9] S. Trasatti and O. Petrii. Real surface area measurements in electrochemistry. *Pure and Applied Chemistry* 63, pp. 711-734, 1991.
- [10] B. Łosiewicz, R. Jurczakowski and A. Lasia. Kinetics of hydrogen underpotential deposition at polycrystalline platinum in acidic solutions. *Electrochim. Acta* 80, pp. 292-301, 2012.
- [11] B. Conway, J. Barber and S. Morin. Comparative evaluation of surface structure specificity of kinetics of UPD and OPD of H at single-crystal Pt electrodes. *Electrochim. Acta* 44, pp. 1109-1125, 1998.
- [12] E. Herrero, K. Franaszczuk and A. Wieckowski. Electrochemistry of methanol at low index crystal planes of platinum: An integrated voltammetric and chronoamperometric study. *J. Phys. Chem.* 98, pp. 5074-5083, 1994.
- [13] J. L. Roberts and D. T. Sawyer. *Electrochemistry for chemists*, Wiley-Interscience; 2nd Ed, 1995.

- [14] A. Januszewska, G. Dercz, J. Piwowar, R. Jurczakowski and A. Lewera. Outstanding catalytic activity of Ultra-Pure platinum nanoparticles. *Chemistry-A European Journal* 19, pp. 17159-17164, 2013.
- [15] M. T. Koper. *Fuel Cell Catalysis: A Surface Science Approach*, Wiley, 2009.
- [16] J. Joo, T. Uchida, A. Cuesta, M. T. Koper and M. Osawa. Importance of acid–base equilibrium in electrocatalytic oxidation of formic acid on platinum. *J. Am. Chem. Soc.* 135, pp. 9991-9994, 2013.
- [17] J. Xu, D. Yuan, F. Yang, D. Mei, Z. Zhang and Y. Chen. On the mechanism of the direct pathway for formic acid oxidation at a Pt (111) electrode. *Physical Chemistry Chemical Physics* 15, pp. 4367-4376, 2013.
- [18] C. A. Rice and A. Wieckowski. "Electrocatalysis of formic acid oxidation," in *Electrocatalysis in Fuel Cells*, Springer-Verlag London, 2013.
- [19] A. Capon and R. Parsons. The oxidation of formic acid on noble metal electrodes: II. A comparison of the behaviour of pure electrodes. *Journal of Electroanalytical Chemistry and Interfacial Electrochemistry* 44, pp. 239-254. 1973.
- [20] D. R. Lycke and S. L. Blair. Fuel cells - exploratory fuel cells - formic acid fuel cells. *Encyclopedia of Electrochemical Power Sources*, pp. 172-181, 2009. DOI: <http://dx.doi.org/10.1016/B978-044452745-5.00864-9>.

- [21] V. Climent, E. Herrero and J. M. Feliu. Electrocatalysis of formic acid and CO oxidation on antimony-modified Pt (111) electrodes. *Electrochim. Acta* 44, pp. 1403-1414, 1998.
- [22] J. Kim and C. K. Rhee. Structural evolution of irreversibly adsorbed Bi on Pt (111) under potential excursion. *Journal of Solid State Electrochemistry* 17, pp. 3109-3114, 2013.
- [23] M. C. Figueiredo, A. Santasalo-Aarnio, F. J. Vidal-Iglesias, J. Solla-Gullón, J. M. Feliu, K. Kontturi and T. Kallio. Tailoring properties of platinum supported catalysts by irreversible adsorbed adatoms toward ethanol oxidation for direct ethanol fuel cells. *Applied Catalysis B: Environmental* 140, pp. 378-385, 2013.
- [24] J. Clavilier, J. Feliu and A. Aldaz. An irreversible structure sensitive adsorption step in bismuth underpotential deposition at platinum electrodes. *Journal of Electroanalytical Chemistry and Interfacial Electrochemistry* 243, pp. 419-433, 1988.
- [25] J. Brugger, B. Tooth, B. Etschmann, W. Liu, D. Testemale, J. Hazemann and P. V. Grundler. Structure and thermal stability of Bi (III) oxy-clusters in aqueous solutions. *Journal of Solution Chemistry* 43, pp. 314-325, 2014.
- [26] E. Leiva, T. Iwasita, E. Herrero and J. M. Feliu. Effect of adatoms in the electrocatalysis of HCOOH oxidation. A theoretical model. *Langmuir* 13, pp. 6287-6293, 1997.
- [27] G. Saravanan, K. Nanba, G. Kobayashi and F. Matsumoto. Leaching tolerance of anodic Pt-based intermetallic catalysts for formic acid oxidation. *Electrochim. Acta* 99, pp. 15-21, 2013.

CHAPTER 4

Electroactivity of PANI supported Pt modified by Bi ad-atoms

4 Electroactivity of PANI supported Pt modified by Bi ad-atoms

4.1 Introduction

Platinum is still the most studied catalyst for oxidation of alcohols and formic acid, although it is limited by CO poisoning and sluggish kinetics towards oxidation reactions. The introduction of one or more metals in order to increase the oxophilicity of a catalyst (Pt) is a common approach for the development of improved materials for fuel cell reactions [1]. Irreversibly adsorbed Bi ad-atom modified Pt has demonstrated superior formic acid electro-oxidation activity. The enhanced electroactivity of Bi modified Pt has been attributed to combined contributions of an electronic effect and a third body effect by Bi [2].

Highly conductive polymers with high surface areas are currently used as fuel cell electrocatalyst supports to provide large electrochemical reaction surfaces [3]. Another aspect of conducting polymers in addition to high surface area is due to their high conductivity (electronic and ionic), controllable morphologies and synergic catalytic effects with precious metal nanoparticles [4]. Polyaniline (PANI) has been extensively applied to support Pt catalysts for the oxidation of single carbon molecules (CH_3OH , HCHO , HCOOH , CO). The use of PANI as a support material leads to a decrease in the amount of precious metal used and allows the improvement of catalytic activity for the oxidation of single carbon molecules [5, 6].

This work describes the electrochemical behavior of irreversibly adsorbed Bi atoms over Pt. As Bi improves the catalytic activity of Pt towards formic acid oxidation, the stability of Bi with respect to positive potential limit and extent of adsorption over Pt as well as the long term activity of Bi-modified Pt has been studied. The electroactivity of Bi modified Pt in conjunction with a polymer (PANI) support effect also has been evaluated.

4.2 Results and Discussion

4.2.1 Characterization of CVs of Bi modified Pt NP and Bi ad-atom stability

Fig 4.1 shows voltammograms of Pt and Pt modified with adsorbed Bi. A typical Pt voltammogram has three regions, the HUPD region, the double layer region and reversible adsorption of hydroxide ($\text{H}_2\text{O} = \text{OH}_{\text{ad}} + \text{e}^- + \text{H}^+$) [7]. The voltammogram of the Bi modified Pt showed a significant decrease in the HUPD peaks. This phenomenon is attributed to the

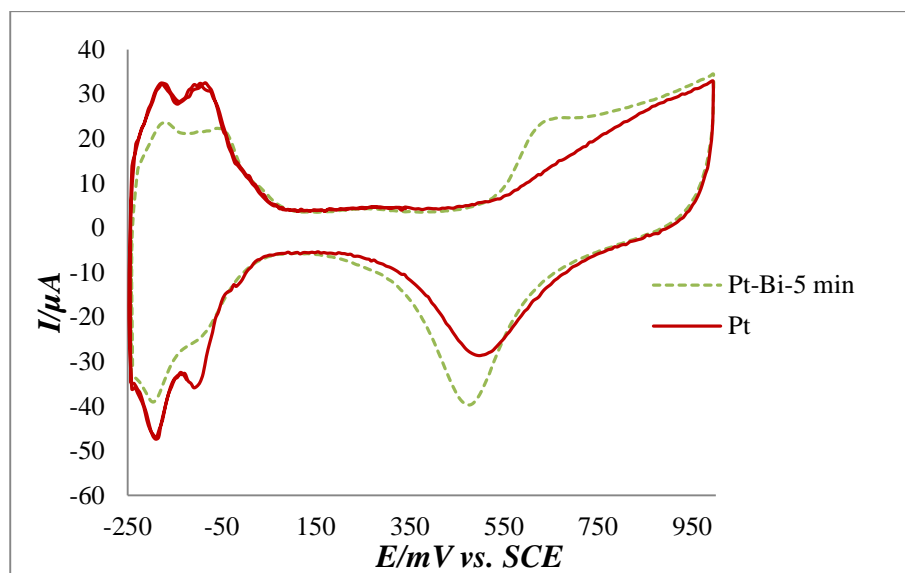


Figure 4.1. Cyclic voltammograms (100 mV s^{-1}) of GC/Pt (Pt NP = $0.64 \mu\text{g}$) and GC/Pt electrodes that has been immersed in $0.1 \text{ mM Bi}_2\text{O}_3 + 0.1 \text{ M H}_2\text{SO}_4$ for 5 min, tested in $0.1 \text{ M H}_2\text{SO}_4$.

site blocking effect of adsorbed Bi over Pt [7, 8] and because of the fact that Bi does not adsorb hydrogen [9]. The modification of Pt with adsorbed Bi did not only decrease the sharpness and intensity of HUPD, it also gave an quasi-reversible redox couple [10]. The quasi-reversible redox couple with an oxidation peak at ca. 630 mV during the anodic scan

and a reduction peak at ca. 485 mV during the cathodic scan is due to oxidation and reduction of adsorbed Bi [11]. The position of the redox couple depends on the surface orientation as it is dependent on the surface structure [12].

Fig 4.2 shows cyclic voltammograms of GC/Pt and GC/Pt modified by Bi adsorbed at various immersion times. The increment in suppression of HUPD peaks corresponded

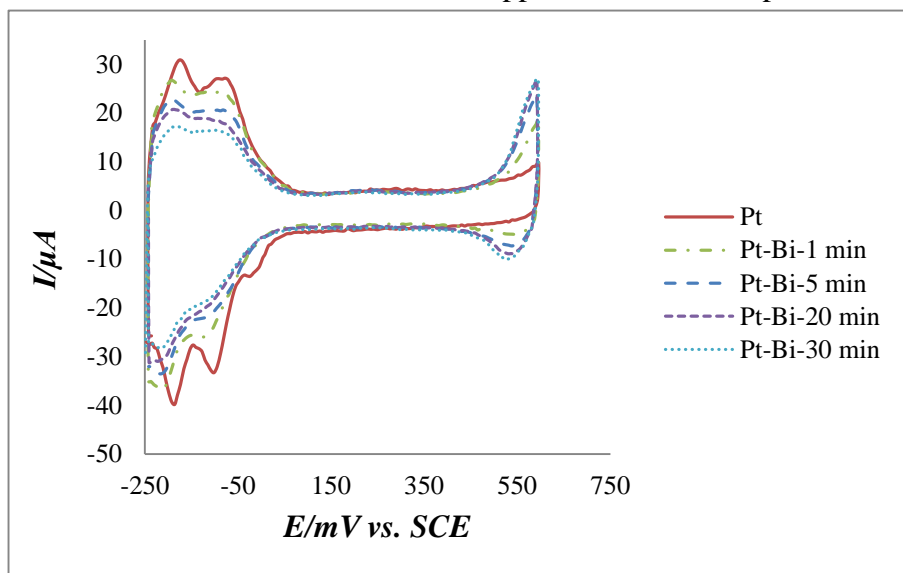


Figure 4.2. Cyclic voltammograms (100 mV s^{-1}) of GC/Pt (Pt NP = $0.64 \mu\text{g}$) electrode that has been immersed in $0.1 \text{ mM Bi}_2\text{O}_3$ for x min and tested in $0.1 \text{ M H}_2\text{SO}_4$ at 100 mV s^{-1} .

with the time of immersion in the solution of Bi. The continuous suppression of HUPD peaks with increasing immersion time shows an increase in the coverage of Pt with Bi ad-atoms. Hence, coverage of Pt with Bi ad-atom is dependent on the immersion time [13]. Moreover, the intensity of the Bi redox couple also corresponded to the immersion time, i.e., the greater the immersion time, the larger the coverage of Pt by Bi ad-atoms and higher the peak intensity of the Bi redox couple. Also, the onset of the oxidation peak for Bi moved

towards negative potential values with the increasing immersion time, or in other words with the increase in the coverage of Bi ad-atoms [14].

The cyclic voltammograms of Bi modified Pt in the HUPD region did not change (there is a change in the intensity but overall shape and position of peaks with respect to potential axis did not change) with immersion time in the solution of Bi. This indicates the nonselective adsorption of Bi over polycrystalline Pt [15].

Fig 4.3 compares the potential dependent behaviour of Bi and Sb modified Pt. The Sb modified Pt cyclic voltammogram has been included for the purpose of comparison of stability with GC/Pt-Bi. In the case of GC/Pt-Bi, the redox couple (Fig 4.1) can not be observed till ca. 500 mV. The redox couple appeared as soon as the scan limit is set above ca. 520 mV. Moreover, the redox couple of Bi ad-atoms is almost reversible until ca. 590 mV (Fig 4.2).

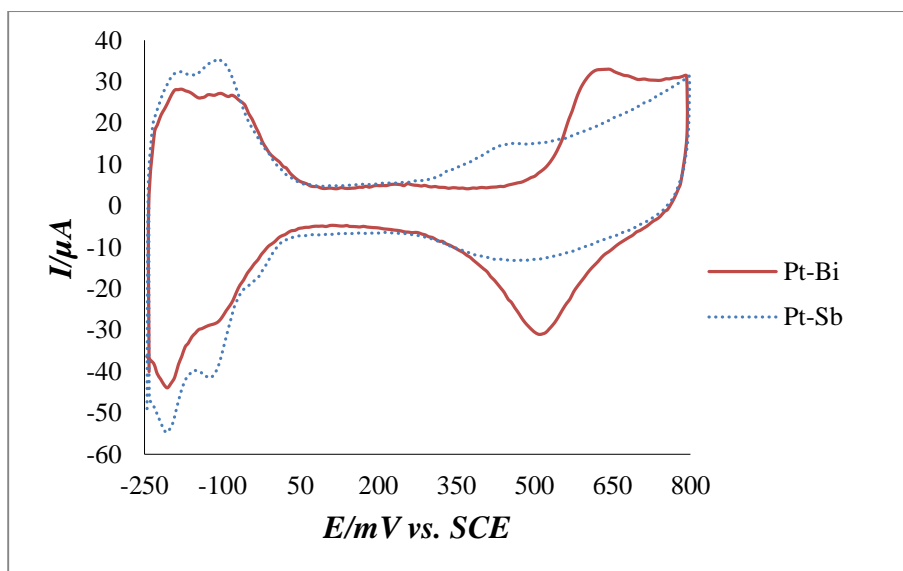


Figure 4.3. Cyclic voltammograms (100 mV s^{-1}) of GC/Pt (Pt NP = $0.64 \mu\text{g}$) electrodes that has been immersed in x min in $0.1 \text{ mM Bi}_2\text{O}_3$ or $0.1 \text{ mM Sb}_2\text{O}_3$ and tested in $0.1 \text{ M H}_2\text{SO}_4$.

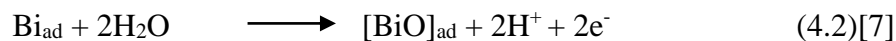
However, the reversibility of the redox couple of Bi ad-atom diminished with increase in the upper potential limit (< 590 mV) as shown in Fig 4.1. Hence, the stability of Bi-ad atom depends on the upper potential limit and it is ca. 590 mV vs. SCE. Therefore, the upper potential limit must be restricted to < ca.590 mV in order to avoid the desorption of Bi ad-atoms from the Pt [14]. In the case of Sb ad-atoms, the redox couple was observed at ca. 450 mV (Fig 4.3). Therefore the upper potential limit for Sb ad-atoms is less than for Bi ad-atoms. Hence, adsorbed Bi over Pt is more stable than Sb ad-atoms.

The stability is dependent on the upper potential limit as shown in the Figures 4.1, 4.2 and 4.3 and desorption is attributed to the formation of unstable oxy-species of Bi and Sb [16]. The onset potential of leaching or desorption of the less noble metals (Bi, Sb) via oxidation corresponds closely to that predicted from Pourbix diagrams [17].

The group V elements (As, Sb and Bi) have s^2p^3 valence shells. Hence, there are five electrons available for bonding. The three p orbitals overlap with three surface Pt atoms, while two s electrons combine with an oxygen atom. Hence, the oxygenated metal species are reduced via solution deposition known as adsorption of ad-atoms over the Pt surface [18]. As far as the stability of Bi ad-atoms is concerned, it is attributed to the $\text{Bi}^0/\text{Bi}^{2+}$ redox couple that gives the reversible peak at 590 mV as shown in Figure 4.2. The surface redox process is related either to



or



An earlier X-ray photoelectron spectroscopy (XPS) study suggested that the irreversibly adsorbed Bi does not change its valence state for different potentials and it remains in its zero valent-state [7]. However, recent XPS data confirms the presence of both metallic and oxy-species of Bi on Pt surfaces [16].

As discussed above, there is no consensus regarding the nature of the peak (redox couple peak at 590 mV in Fig 4.2). The original proposition was based on the chemical equations (4.1, 4.2) [19], while XPS data suggested otherwise (zerovalent state of Bi). Ultra high vacuum studies suggest that the charge under the peak at 590 mV in Fig 4.2 is not due to the $\text{Bi}^0/\text{Bi}^{2+}$ redox couple. It has been attributed to anion adsorption/desorption (e.g., OH_{ad}) and this is the surface process creating the pseudocapacitance of the peak previously regarded as a redox couple of Bi [7].

The adsorption of ad-atoms is in the form of islands randomly distributed without any preference for site on the polycrystalline Pt nanoparticles surface. There are always void spaces between the islands of Bi ad-atoms and the morphology does not change with oxidation of the Bi ad-atoms except the addition of oxygen species (most probably O^{2-} or OH^-) [20]. The induced adsorption of OH_{ad} onto Pt sites neighbouring the Bi ad-atom has been proposed at a potential that is lower than that for OH_{ad} on the unmodified Pt surface [7]. The XPS data also confirms the presence of metallic Bi and its oxy species on the Pt surface after immersion in Bi solution under open-circuit conditions [16]. X-ray diffraction (XRD) analysis of the Bi ad-atom modified Pt showed that there is no alloy formation between the two metals and Bi ad-atoms merely exist as an adsorbed species at the surface of Pt [2].

To summarize the above discussion, it can be concluded that the Bi ad-atoms exist as metallic Bi along with oxygenated species after the immersion of Pt in Bi solution. The metallic Bi atoms are reversibly oxidized (590 mV) and Bi ad-atoms are stable over Pt. However, if the upper potential is increased above 590 mV, the Bi ad-atoms are oxidized irreversibly and desorb from the surface of Pt. The presence of adsorbed Bi at the surface of Pt induces the adsorption of OH_{ad} over the neighbouring Pt sites at lower potential than the oxidation of Pt itself. The amount of adsorbed Bi increases with the immersion time. The charge under the HUPD decreases with an increase in the adsorption of Bi ad-atoms over Pt and the onset potential of the Bi redox couple decreases (towards negative potential) with increase in the immersion time.

4.2.2 Electroactivity of Bi modified Pt versus immersion time

Fig 4.4 shows the relationship between the coverage of Pt by Bi ad-atoms and immersion time in an acidic solution of Bi. At about one min of immersion in Bi solution, there is an approximately 15% coverage of Pt by Bi ad-atoms. As immersion time increases, coverage increases steadily until it reaches a value of about 44% at an immersion time of 30 min. The coverage value corresponding to an immersion time of 40 min was lower than for an immersion time of 30 min and this is likely due to experimental error.

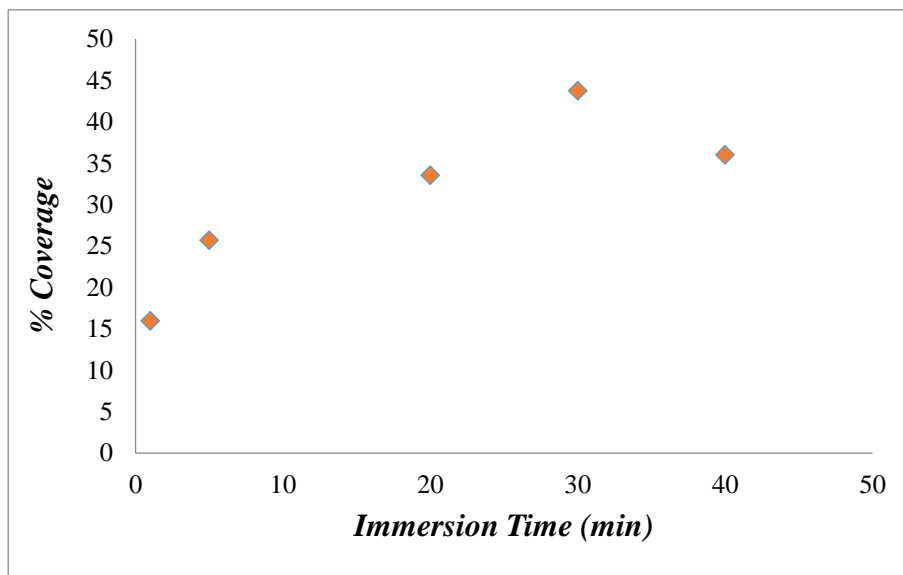


Figure 4.4. Relationship between Pt coverage by Bi ad-atoms and immersion time.

The maximum coverage achieved at an immersion time of 30 min was ca. 44%. We could not achieve higher coverage and this may be explained by the lack of availability of oxygenated Bi species at the low pH value of 0.1 mM Bi₂O₃ dissolved in 0.1 M H₂SO₄. The lack of availability of oxygenated species at low pH values can be justified by Figure 4.5 which represents the speciation of Bi in acidic solution. We know that the pH of the solution of 0.1 mM Bi dissolved in 0.1 M H₂SO₄ is approximately 1. As shown in Figure 4.5, at pH ≈ 1 and 0.1 mM Bi(III), the corresponding oxygenated Bi species concentration will be very low. As the pH value increases, the corresponding concentration of hydroxide species of Bi increases.

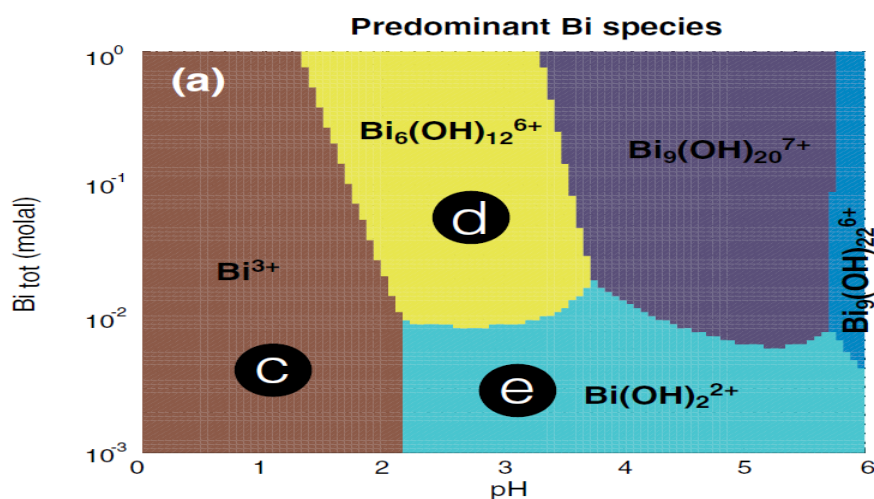


Fig 4.5. Speciation of Bi(III) in acidic solution (figure used with permission) [21].

The lack of oxygenated species at $\text{pH} \approx 1$ was further investigated by using solutions of slightly different pH. Figure 4.6 shows voltammograms of Bi modified Pt for formic acid oxidation. The GC electrode drop coated with Pt was immersed for 5 min in a solution of 0.1 mM Bi_2O_3 in 0.1 M H_2SO_4 and a solution of 0.1 mM Bi_2O_3 in 0.5 M H_2SO_4 . The results for the oxidation of formic acid are shown in Figure 4.6. There is a clear difference in the performance of the two electrodes. The Pt modified with Bi in 0.5 M H_2SO_4 gave only ca. 359 μA at 350 mV for formic acid oxidation, while Pt modified with Bi dissolved in 0.1 M H_2SO_4 gave a current of 1770 μA at 350 mV. Also, there is a difference in the onset potential for the two electrodes for formic acid oxidation. The difference in the onset potential and peak current for formic oxidation for the two electrodes (Pt modified with Bi dissolved in 0.1 M H_2SO_4 or 0.5 M H_2SO_4) can be attributed to the amount of Bi adsorbed at the Pt surface (see below) and the amount of Bi adsorbed therefore appears to be dictated

by the amount of oxygenated Bi species at different pH values. This has been subsequently confirmed by another group member [22].

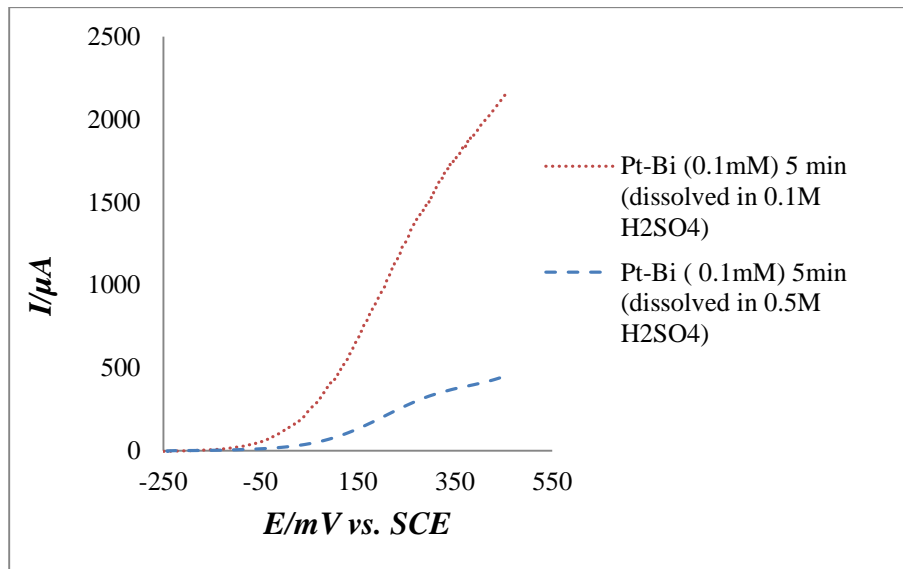


Fig 4.6. Second anodic scan of voltammograms of GC/Pt (Pt NP 1.25 μL = 0.64 μg) electrodes that has been immersed for 5 min in 0.1 mM Bi_2O_3 dissolved in 0.1 M H_2SO_4 and 0.5 M H_2SO_4 and tested in 0.1 M H_2SO_4 + 0.5 M HCOOH at 10 mV s^{-1} .

Fig 4.7 shows voltammograms for oxidation of formic acid at other Bi modified Pt electrodes and a Pt electrode. The Pt electrodes were modified by immersion in Bi solution for different times. The purpose of the experiment was to establish the role of Bi modified Pt for formic acid oxidation and to find an optimum time of immersion for the modification of Pt with Bi ad-atoms.

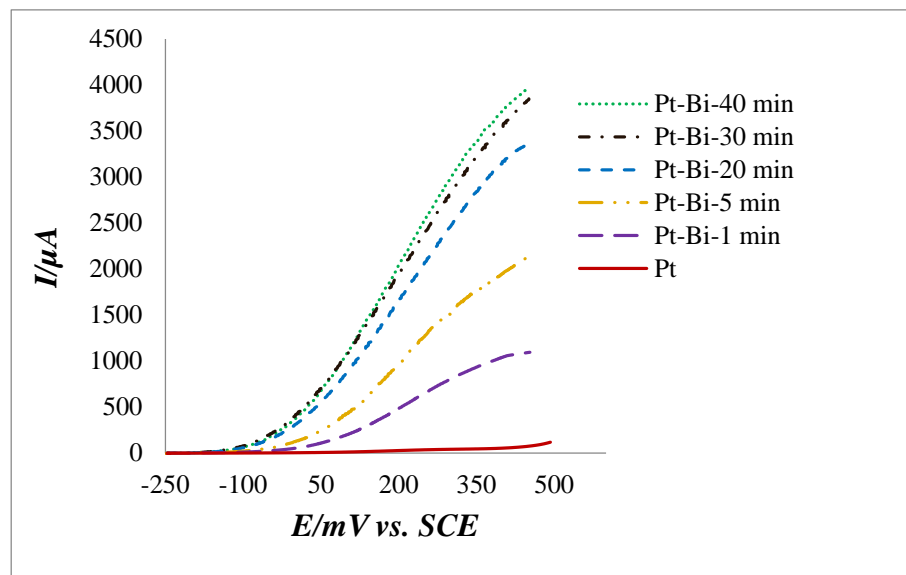


Fig. 4.7. Second anodic scan of voltammograms (10 mV s^{-1}) of GC/Pt (Pt NP = $0.64 \text{ } \mu\text{g}$) electrodes that have been immersed for x min in $0.1 \text{ mM Bi}_2\text{O}_3$ dissolved in $0.1 \text{ M H}_2\text{SO}_4$ and tested in $0.1 \text{ M H}_2\text{SO}_4 + 0.5 \text{ M HCOOH}$.

In comparison to the formic acid oxidation currents for the Pt electrode, the Bi modified electrodes gave high currents at low potential values. The formic acid oxidation current values also increased with increasing immersion time of the Pt electrode in the Bi solution which corresponds to an increasing coverage of Bi adsorbed over the Pt surface. Hence, formic acid oxidation efficiency depends on the coverage of Pt by Bi [13]. Beside peak current values, there is a clear difference in the onset potential values for formic acid oxidation for the Bi modified Pt electrodes with respect to the Pt electrode. The onset potential values for formic acid oxidation decreased with increasing immersion time. This reduction in the overpotential indicates the promotion of the dehydrogenation (direct) pathway for formic acid oxidation [2]. A decrease in the onset potential led to peak formic acid oxidation rates at potentials close to 500 mV. Hence, the potential window for formic

acid oxidation by a Bi modified electrode was set to 500 mV instead of 800 mV as in the case of Pt electrodes. The decrease in the potential window from 800 mV to 500 mV was also necessary to avoid the oxidation of Bi ad-atoms that may lead to their desorption [14].

The onset potential for oxidation of Bi ad-atoms was ca. 480 mV (Fig 4.3). A part of formic acid oxidation occurred at partially oxidized Bi-ad atoms. According to the literature, dehydration and dehydrogenation of formic acid cannot take place at reduced Bi ad-atoms; instead, partially oxidized Bi can facilitate an oxidation path that does not involve poisoning of the catalyst [13]. A shift in the onset potential to lower potential values due to the inhibition of poisoning (CO formation) is of key importance for practical applications of fuel cells. A higher power density can be achieved by a fuel cell with an anode that could work at low potential values which favors the stabilization of adsorbed ad-atoms on the Pt surface, resulting in prolonged catalyst life [23].

Adsorption of Bi on Pt is dictated by the surface structure and one Bi ad-atom takes three Pt sites [2]. The adsorbed Bi does not form a closely packed layer over the Pt surface and hence provides reactant molecules direct access to Pt atoms in an electrode reaction [2]. Ad-atoms block a fraction of the Pt surface and inhibit poison formation [24]. In other words, adsorption of Bi on the Pt surface creates isolated regions of Pt and this gives the Pt surface an ensemble size that decreases as the coverage of Bi increases. According to the third body effect phenomenon, a Pt site nearby a Bi ad-atom is necessary for the oxidation of formic acid [24]. Hence a variation in ensemble size plays a critical role for the oxidation reaction of formic acid [13]. Therefore, as the immersion time was increased (Fig 4.7), the coverage increased (less Pt sites are available for poisoning by CO) corresponding to a

decreased ensemble size and high activity for formic acid oxidation. In the literature, an ensemble size of diameter of 2 nm is said to be a critical size for the dehydration pathway of formic acid electro-oxidation by Bi modified Pt electrocatalysts [2, 13]. Also, theoretically it is suggested that an increase in Bi coverage increases the direct pathway of formic acid electro-oxidation by electronic modification of Pt [2].

Fig 4.8 shows the relationship between Bi coverage and Bi modified Pt electroactivity for the electro-oxidation of formic acid. We can see that there is a large improvement of electroactivity for a small coverage of Bi (12%).

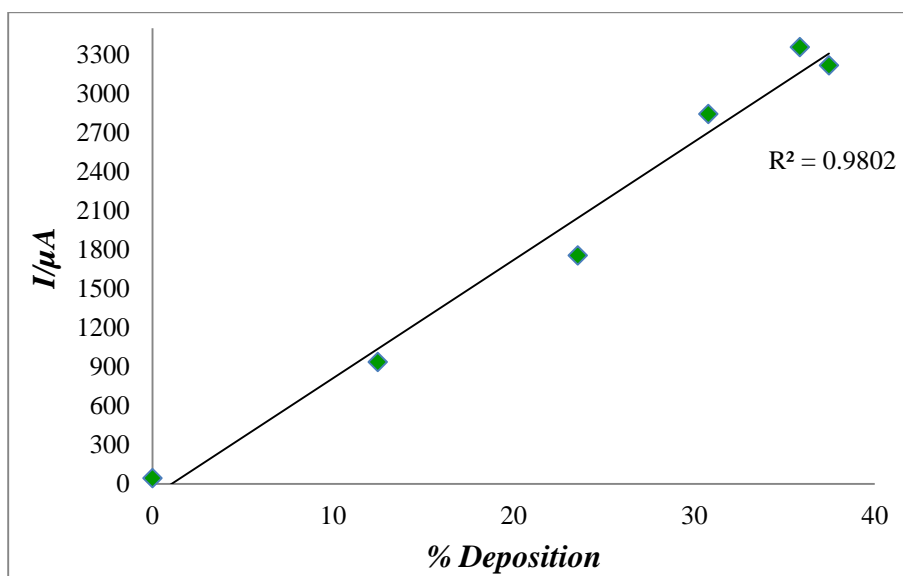


Fig. 4.8. % Coverage (Bi) vs electroactivity of Bi modified Pt.

According to a theoretical model [24] devised for the electro-oxidation of formic acid in sulfuric acid for Bi modified Pt, Bi is considered to be randomly deposited on the Pt surface and the activity of the electrode surface is directly proportional to paired Pt-Bi sites. At low Bi coverage, there is a significant increase in the electroactivity as new pairs

Pt-Bi are created. The increase in activity continues linearly with coverage until there is a loss (high coverage of Bi) of free Pt sites required for the oxidation reaction of formic acid. High coverage will not create new pairs; instead there is a loss of Pt sites [25]. However, we see just a linear relationship between coverage and activity (Fig 4.8) as we could not achieve high enough coverage to observe the loss of activity.

4.2.3 Electroactivity of Pt modified by ad-atoms for formic acid oxidation

Fig 4.9 shows electroactivity for formic acid oxidation versus coverage (%) of ad-atoms (Bi, Sb) on Pt.

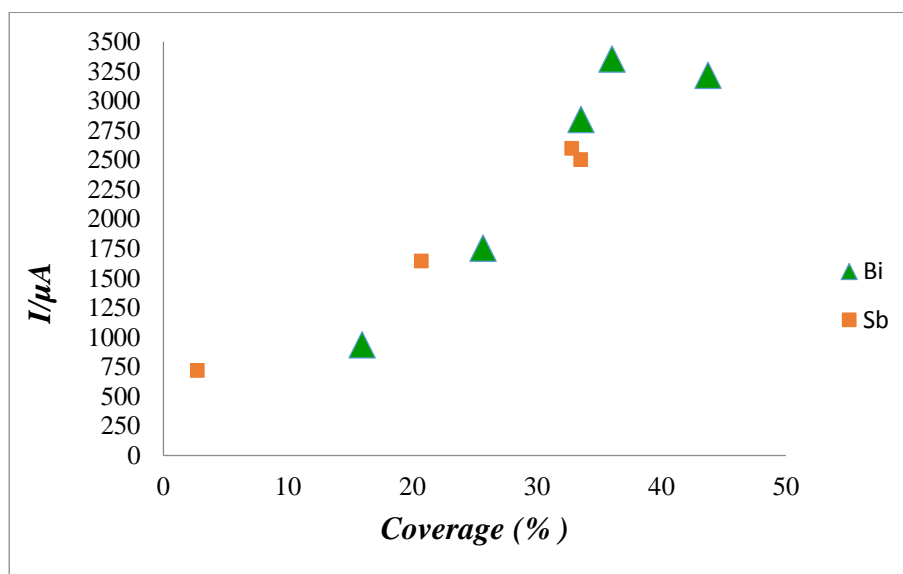


Fig 4.9. The electroactivity for formic acid oxidation versus coverage (%) of Pt by Bi and Sb ad-atoms.

The data for the Sb ad-atoms have been added for comparison with Bi. There is a difference between the coverage values of Bi and Sb ad-atoms on the surface of the Pt. The maximum coverage obtained for Sb was about 33%, while for Bi the highest coverage was

about 44%. Also, in the beginning at 5 min deposition, the coverage values differ even more as it is only 3% for Sb, while Bi gave 16% coverage. The difference in the coverage of the Pt by Bi and Sb under the same conditions such as pH, metal solution concentration and an immersion time could be explained by the nature of the adsorption phenomenon of the two metal atoms (Sb, Bi). The adsorption depends on the crystal structure of the substrate, nature of the adsorbent and its atomic radius. The atomic radius governs the site requirement for an ad-atom over the substrate. We know that the atomic radii of Sb and Bi are 1.61 Å and 1.82 Å respectively [18]. The atomic radius of Pt is 1.38 Å. Hence, it is obvious that the ad-atoms (Bi, Sb) would be adsorbed over more than one Pt site. The observed values for the Bi and Sb ad-atoms are 2.5 and 3.0 Pt site [18]. The probability of finding 2.5 Pt (for Sb ad-atom) sites may be slightly more than 3.0 Pt (for Bi ad-atom) [18]. However, due to the difference in atomic radii, the lattice misfit may affect the adsorption phenomenon. The contribution of lattice misfit is obvious in the case of crystal structures of Pt such as (Pt(111), Pt(100), Pt(320), Pt(321)) as different crystal structures give different values of charge and hence the number of sites required for the adsorption of Sb ad-atoms [26]. A detailed morphology study of Bi and Sb modified Pt (Pt NP) could be helpful to find out the reason for the different coverage values.

4.2.4 Optimum metal solution concentration for adsorption of Bi over Pt NP

In order to find an optimum concentration of metal solution (Bi), different concentrations of Bi_2O_3 were used at a constant immersion time (5 min) followed by testing the electrodes for formic acid oxidation. The resultant voltammograms are shown in Fig

4.10. The highest concentration of Bi_2O_3 used was 0.1 mM as it was not possible to dissolve higher amounts of Bi_2O_3 in 0.1 M H_2SO_4 . The Pt electrode modified with 0.1 mM Bi_2O_3 gave the highest current and lowest onset potential for oxidation of formic acid compared to the other concentrations of metal oxide (0.001 mM Bi_2O_3 and 0.01 mM Bi_2O_3 dissolved in 0.1 M H_2SO_4). Hence, the optimum and highest possible concentration of metal oxide in 0.1 M H_2SO_4 for modification of Pt electrode for formic acid oxidation is 0.1 mM Bi_2O_3 .

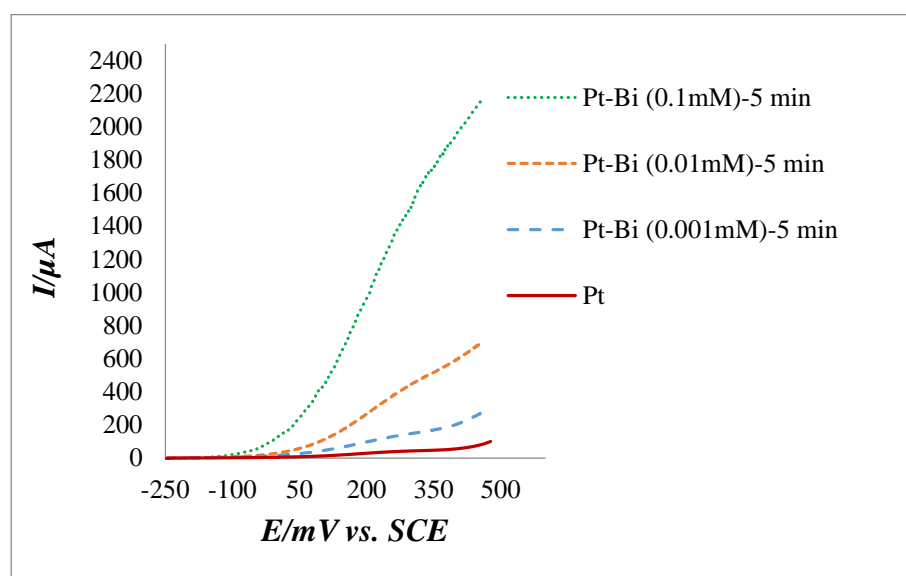


Fig. 4.10. Second anodic scan of voltammograms (10 mV s^{-1}) of GC/Pt (Pt NP = $0.64 \mu\text{g}$) electrodes that has been immersed for 5 min in x mM Bi_2O_3 dissolved in 0.1 M H_2SO_4 and tested in 0.1 M $\text{H}_2\text{SO}_4 + 0.5 \text{ M HCOOH}$.

4.2.5 Constant potential evaluation of Bi modified Pt for formic acid oxidation

Chronoamperometry (CA) results are used to assess the resistance of catalysts to poisoning and the stability of the catalyst for an extended period of time for practical applications. As shown in Fig 4.11 both types of electrodes (Pt modified with Bi and Sb) show high currents compared to Pt alone. The higher initial current may be due to rapid

change to an applied potential [27]. There is a slight difference in the electroactivity of Bi and Sb modified Pt electrodes and this difference could be attributed to the difference in the coverage of Bi and Sb ad-atoms (Fig 4.9). The continuous decrease in the current with time (Fig 4.11) could be due to poisoning of the Pt sites and leaching of the ad-atoms (Sb, Bi). The loss of ad-atoms (leaching) at low potential values compared to observed oxidation potential values for Bi and Sb in Fig 4.3 could be attributed to the presence of formic acid in the solution ($\text{HCOOH} + \text{H}_2\text{SO}_4$) [17, 25]. The ad-atoms are lost via leaching of less noble metals (Sb, Bi) leaving behind a Pt rich surface susceptible for the poisoning [17, 28].

The CA experiments confirmed the high activity of Bi or Sb modified Pt. The high activity in constant potential experiments and in cyclic voltammetric experiments shown by the ad-atom modified Pt catalysts originates from the ensemble effect and a continuous decrease in activity shown in CA experiments is due to leaching of adsorbed ad-atoms ($\text{HCOOH} + \text{H}_2\text{SO}_4$) [17, 25].

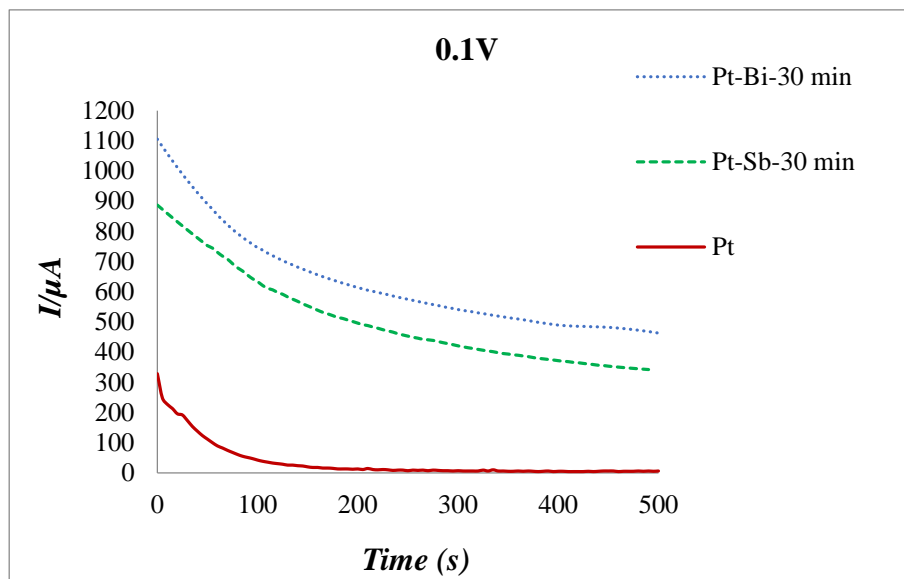


Fig. 4.11. Chronoamperometry at 100 mV for GC/Pt and GC/Pt immersed in 0.1 mM Sb_2O_3 / 0.1 mM Bi_2O_3 versus time and tested in 0.1 M H_2SO_4 + 0.5 M HCOOH .

4.2.6 Formic acid oxidation by Pt NP modified by (Bi + Sb)

Fig 4.12 shows voltammograms for formic acid oxidation at Pt, and Pt modified by both Bi and Sb ad-atoms. The purpose of these experiments was to study the combined (Bi+Sb) ad-atom modification effect of Pt towards formic acid oxidation. As discussed above, Bi and Sb ad-atoms improve the catalytic activity of Pt via a third body effect through ensemble formation and probably via an electronic effect (modification of electronic properties of Pt to increase the electroactivity). The combined effect of Bi and Sb ad-atoms for the improvement Pt activity has been demonstrated in Fig 4.12 as we can see that there is a clear difference in the onset potential between Bi (ca. -150 mV) modified Pt and Bi+Sb (onset potential ca. -210 mV) modified Pt. Although the maximum current is almost the same in both cases (Fig 4.12), the negative shift of the onset potential to ca. -

210 mV for (Bi+Sb modified Pt) clearly shows the improvement in electrocatalytic activity for formic acid oxidation.

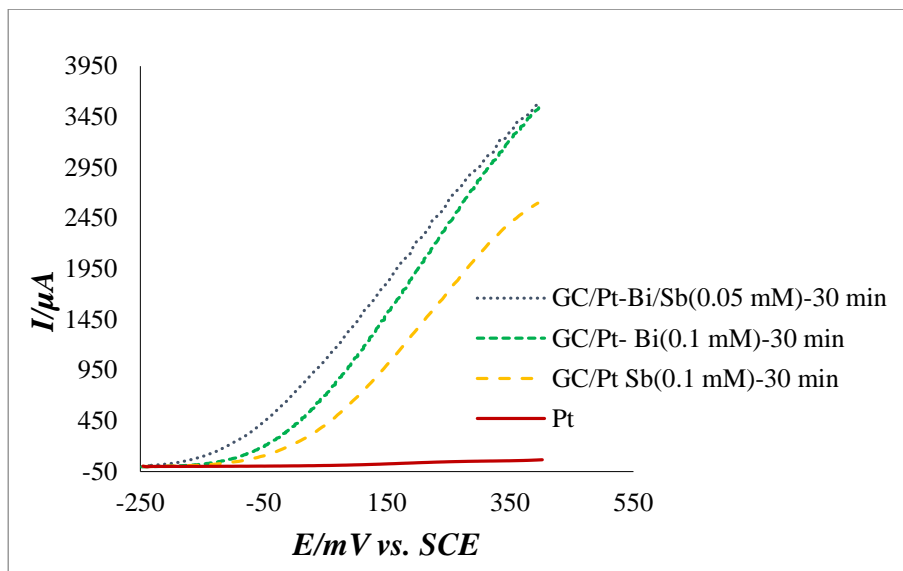


Fig. 4.12. Second anodic scan of voltammograms (10 mV s^{-1}) of GC/Pt (Pt NP = $0.64 \mu\text{g}$) and GC/Pt electrodes immersed for 30 min in $0.1 \text{ mM Bi}_2\text{O}_3$, $0.1 \text{ mM Sb}_2\text{O}_3$ and $0.05 \text{ mM (Bi}_2\text{O}_3 + \text{Sb}_2\text{O}_3)$ dissolved in $0.1 \text{ M H}_2\text{SO}_4$ and tested in $0.1 \text{ M H}_2\text{SO}_4 + 0.5 \text{ M HCOOH}$.

4.2.7 PANI support effect for Pt and Bi modified Pt for formic acid oxidation

Fig 4.13 shows cyclic voltammograms of GC/Pt and GC/PANI/Pt electrodes in $0.1 \text{ M H}_2\text{SO}_4$. The presence of PANI is clearly indicated by peaks at ca. 120 mV and ca. 690 mV along with enhanced current above 0 mV. The peaks above 0 mV for cyclic voltammograms of PANI are the electro-oxidation peaks of PANI. Peaks under 0 mV represent the HUPD region [4, 29]. In order to avoid the degradation of PANI by electro-oxidation, the positive potential was set to 800 mV for the blanks (Fig 4.13) and an even lower potential value (400 mV) for the study of support effect for ad-atom modified Pt (Fig 4.14).

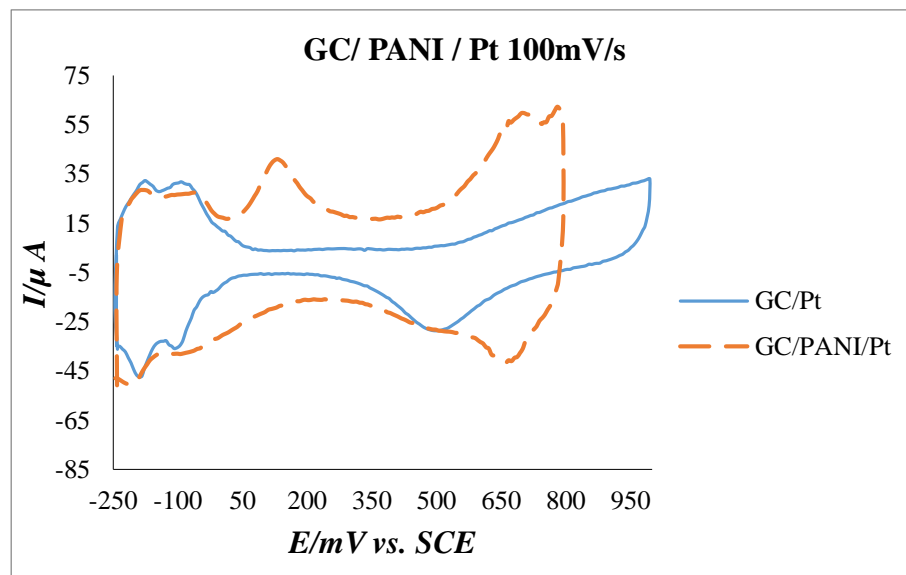


Fig. 4.13. Cyclic voltammograms (100 mV s^{-1}) of GC/Pt and GC/PANI/Pt electrodes in $0.1 \text{ M H}_2\text{SO}_4$.

The presence of PANI did not have a significant effect on the HUPD region. This probably indicates that the utilization of the Pt active area being similar to Pt without any support material underneath. The only way to observe the presence of a third body effect or ensemble effect is the suppression of the HUPD peaks as observed in the case of ad-atoms. A slight decrease in the anodic HUPD peaks may be a misleading indicator of a decrease in electroactive area of the electrode, since experimentally calculated (via Cu underpotential deposition) electroactive area values were higher for electrodes with a PANI support than GC electrodes drop coated with Pt NP [30]. Hence, the support material can increase the utilization of the area of the Pt [4, 30].

Fig 4.13 shows linear sweep voltammograms (LSVs) for the GC/Pt and GC/PANI/Pt electrodes in $0.1 \text{ M H}_2\text{SO}_4$ and 0.5 M HCOOH . There is a significant difference in the peak heights of voltammograms of the two electrodes.

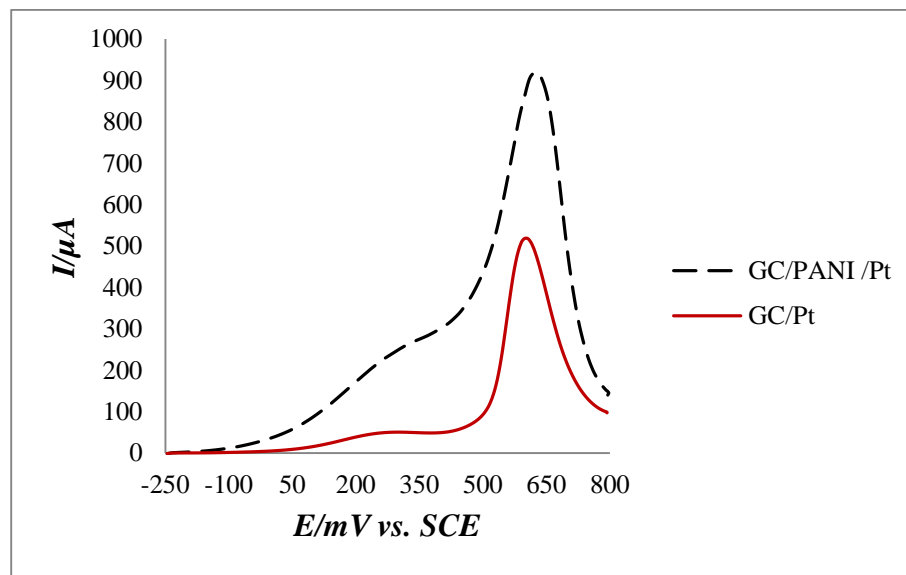


Fig. 4.14. Second anodic scan of voltammograms (10 mV s^{-1}) of GC/Pt and GC/PANI/Pt electrodes in $0.1 \text{ M H}_2\text{SO}_4 + 0.5 \text{ M HCOOH}$.

The peak at ca. 300 mV corresponds to the direct pathway for oxidation of formic acid for the GC/Pt electrode and the corresponding peak for the GC/PANI/Pt electrode has roughly 5 times higher current. There is also a significant difference in the onset potential for the direct pathway which is ca. 0 mV for GC/Pt while the onset potential for the GC/PANI/Pt is ca. -100 mV. Similarly, the peaks for the indirect pathway of formic acid oxidation have different current values, although there is almost no difference in the onset potential. The difference in the peak heights that corresponds to the current values strongly suggests a synergic effect between the polymer support and Pt nanoparticles [30]. The origin of the synergic effect between Pt NP and the polymer support is believed to be a mechanistic and/or an electronic effect [4]. It may also be due to better dispersion and/or enhanced transport properties [5]. The porous structure, high surface area, and high electrical conductivity of the polymer make it possible to shuttle electrons through the

polymer chains along with dispersion of the metal nanoparticles. All these effects improve the overall catalytic activity as demonstrated in Figure 4.14 [31].

In Figure 4.13, we can see that there is a higher current for the indirect pathway for oxidation of formic acid for the GC/Pt/PANI electrode compared to the GC/Pt electrode. This indicates that the support effect of the polymer does not inhibit poisoning of Pt by CO, instead it facilitates the oxidation of CO. Hence, a bifunctional mechanism involving adsorption of OH to oxidize CO cannot be ruled out. Therefore, the support effect of PANI could be explained by both electronic and bifunctional mechanisms [29].

Fig 4.14 shows LSVs of GC/Pt, GC/PANI/Pt, as well as Bi modified GC/Pt and GC/PANI/Pt for formic acid oxidation at 10 mV s^{-1} . The purpose of these experiments was to test the support effect of the polymer along with ad-atom modified Pt (Bi modified GC/PANI/Pt) for formic acid oxidation. The positive potential voltage was set to 350 mV to avoid desorption of ad-atom and the oxidation of PANI. Comparing peak currents for the direct pathway of oxidation of formic acid by GC/PANI/Pt and Bi modified GC/PANI/Pt, there is an improvement of 4 times in the value of peak current at ca. 350 mV for Bi modified GC/PANI/Pt versus GC/PANI/Pt and this improvement can be attributed to the catalytic effect of Bi modified Pt as discussed previously.

A combined or synergic effect of Bi modified Pt and the polymer support can be observed in Figure 4.13 when comparing LSVs peaks for formic acid oxidation by Bi modified GC/Pt and Bi modified GC/PANI/Pt. The onset potential is similar for both the electrodes while there is a considerable difference in the peak current (Bi modified GC/Pt

$\approx 930 \mu\text{A}$, Bi modified GC/PANI/Pt $\approx 1300 \mu\text{A}$ at ca. 350 mV). This clearly shows the improvement in electroactivity for Bi modified Pt having PANI as support.

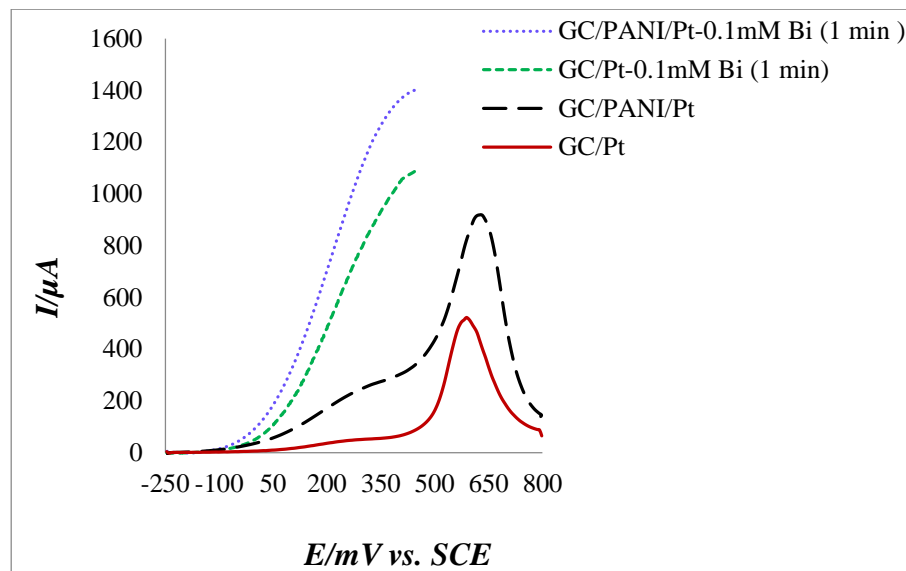


Fig.4.15. Second anodic scan of voltammograms of GC/Pt, GC/PANI/Pt, Bi modified GC/Pt and Bi modified GC/PANI/Pt electrodes in 0.1 M H_2SO_4 + 0.5 M HCOOH at 10 mV s^{-1} .

4.3 Conclusions

This work reports the enhancement of electroactivity for the oxidation of formic acid by modification of Pt nanoparticles with Bi ad-atoms. The presence of Bi ad-atoms increases the Pt activity via a third body effect (impeding poisoning of Pt by CO) and possibly by an electronic effect [1]. The difference in the catalytic activity of Bi modified Pt relative to Pt was roughly 80 times for oxidation of formic acid in an acidic medium (0.1 M H₂SO₄). Modification of Pt was carried out by a solution immersion method at open circuit potential and there was a linear relationship between the immersion time and adsorption of Bi on the surface of the Pt. There was a linear correlation between the electroactivity for formic acid oxidation and coverage (%) of Bi ad-atoms on the Pt. The optimum time for immersion was found to be 40 min. Moreover, the optimum concentration of the metal solution for deposition was found to be 0.1 mM Bi₂O₃ for 0.1 M H₂SO₄ solutions. Also the acid solution molarity plays a critical role for deposition. A higher pH acid solution (0.1 M H₂SO₄), was found to be better than 0.5 M H₂SO₄. This has been attributed to the higher concentration of oxygenated metal species available to be adsorbed onto the Pt. The maximum coverage (%) obtained was about 43%. The stability of the ad-atoms of Bi was also evaluated and it was found that the stability of ad-atoms is highly dependent on the applied positive potential limit. The positive potential limit should not be more than 550 mV vs. SCE in order to avoid desorption.

PANI was used as a polymer support with both Pt and Pt modified with Bi ad-atoms and showed improvement in the electroactivity for formic acid oxidation. PANI improved both the onset potential as well as the peak current for formic acid oxidation, when used

with Pt. However, in the case of Bi ad-atom modified Pt, PANI only showed an increase in the peak current for formic acid oxidation.

4.4 References

- [1] M. C. Figueiredo, R. M. Arán-Ais, J. Feliu, K. Kontturi and T. Kallio. Pt catalysts modified with Bi: Enhancement of the catalytic activity for alcohol oxidation in alkaline media. *Journal of Catalysis* 312, pp. 78-86, 2014.
- [2] A. S. Bauskar and C. A. Rice. Spontaneously Bi decorated carbon supported Pt nanoparticles for formic acid electro-oxidation. *Electrochim. Acta* 93, pp. 152-157, 2013.
- [3] S. Sharma and B. G. Pollet. Support materials for PEMFC and DMFC electrocatalysts—a review. *J. Power Sources* 208, pp. 96-119, 2012.
- [4] R. B. Moghaddam and P. G. Pickup. Support effects on the oxidation of formic acid at Pd nanoparticles. *Electrocatalysis* 2, pp. 159-162, 2011.
- [5] R. B. Moghaddam and P. G. Pickup. Support effects on the oxidation of methanol at platinum nanoparticles. *Electrochemistry Communications* 13, pp. 704-706, 2011.
- [6] H. Zhou, S. Jiao, J. Chen, W. Wei and Y. Kuang. Effects of conductive polyaniline (PANI) preparation and platinum electrodeposition on electroactivity of methanol oxidation. *J. Appl. Electrochem.* 34, pp. 455-459, 2004.
- [7] T. Schmidt, B. Grgur, R. Behm, N. Markovic and P. Ross Jr. Bi adsorption on Pt (111) in perchloric acid solution: A rotating ring–disk electrode and XPS study. *Physical Chemistry Chemical Physics* 2, pp. 4379-4386, 2000.

- [8] S. P. Smith and H. D. Abruña. Structural effects on the oxidation of HCOOH by bismuth modified Pt (111) electrodes with (110) monatomic steps. *J Electroanal Chem* 467, pp. 43-49, 1999.
- [9] J. D. Lović, D. V. Tripković, K. Đ Popović, V. M. Jovanović and A. V. Tripković. Electrocatalytic properties of Pt-Bi electrodes towards the electrooxidation of formic acid. *Journal of the Serbian Chemical Society* 78, pp. 1189-1202, 2013.
- [10] M. C. Figueiredo, A. Santasalo-Aarnio, F. J. Vidal-Iglesias, J. Solla-Gullón, J. M. Feliu, K. Kontturi and T. Kallio. Tailoring properties of platinum supported catalysts by irreversible adsorbed adatoms toward ethanol oxidation for direct ethanol fuel cells. *Applied Catalysis B: Environmental* 140, pp. 378-385, 2013.
- [11] A. S. Bauskar and C. A. Rice. Spontaneously Bi decorated carbon supported Pd nanoparticles for formic acid electro-oxidation. *Electrochim. Acta* 107, pp. 562-568, 2013.
- [12] J. Feliu, A. Fernandez-Vega, A. Aldaz and J. Clavilier. New observations of a structure sensitive electrochemical behaviour of irreversibly adsorbed arsenic and antimony from acidic solutions on Pt (111) and Pt (100) orientations. *Journal of Electroanalytical Chemistry and Interfacial Electrochemistry* 256, pp. 149-163, 1988.
- [13] J. Kim and C. K. Rhee. Ensemble size estimation in formic acid oxidation on Bi-modified Pt (111). *Electrochemistry Communications* 12, pp. 1731-1733, 2010.
- [14] A. López-Cudero, F. J. Vidal-Iglesias, J. Solla-Gullón, E. Herrero, A. Aldaz and J. M. Feliu. Formic acid electrooxidation on Bi-modified polyoriented and preferential (111) Pt nanoparticles. *Physical Chemistry Chemical Physics* 11, pp. 416-424, 2009.

- [15] E. Bertin, S. Garbarino and D. Guay. Formic acid oxidation on Bi covered Pt electrodeposited thin films: Influence of the underlying structure. *Electrochim. Acta* 134, pp. 486-495, 2014.
- [16] V. Pautienienė, L. Tamašauskaitė-Tamašiūnaitė, A. Sudavičius, G. Stalnionis and Z. Jusys. Spontaneous Bi-modification of polycrystalline Pt electrode: Fabrication, characterization, and performance in formic acid electrooxidation. *Journal of Solid State Electrochemistry* 14, pp. 1675-1680, 2010.
- [17] J. Lović, M. Obradović, D. Tripković, K. D. Popović, V. Jovanović, S. L. Gojković and A. Tripković. High activity and stability of Pt₂Bi catalyst in formic acid oxidation. *Electrocatalysis* 3, pp. 346-352, 2012.
- [18] N. Furuya and S. Motoo. Arrangement of ad-atoms of various kinds on substrates: Part I. platinum substrate. *Journal of Electroanalytical Chemistry and Interfacial Electrochemistry* 98, pp. 189-194, 1979.
- [19] J. Clavilier, J. Feliu and A. Aldaz. An irreversible structure sensitive adsorption step in bismuth underpotential deposition at platinum electrodes. *Journal of Electroanalytical Chemistry and Interfacial Electrochemistry* 243, pp. 419-433, 1988.
- [20] J. Kim and C. K. Rhee. Structural evolution of irreversibly adsorbed Bi on Pt (111) under potential excursion. *Journal of Solid State Electrochemistry* 17, pp. 3109-3114, 2013.
- [21] J. Brugger, B. Tooth, B. Etschmann, W. Liu, D. Testemale, J. Hazemann and P. V. Grundle. Structure and thermal stability of Bi (III) oxy-clusters in aqueous solutions. *Journal of Solution Chemistry* 43, pp. 314-325, 2014.

- [22] E. N. El Sawy, M. A. Khan and P. G. Pickup. Factors affecting the spontaneous adsorption of Bi (III) onto Pt and PtRu nanoparticles. *Appl. Surf. Sci.* 364, pp. 308-314, 2016.
- [23] Q. Chen, Z. Zhou, F. J. Vidal-Iglesias, J. Solla-Gullón, J. M. Feliu and S. Sun. Significantly enhancing catalytic activity of tetrahedral Pt nanocrystals by Bi adatom decoration. *J. Am. Chem. Soc.* 133, pp. 12930-12933, 2011.
- [24] E. Leiva, T. Iwasita, E. Herrero and J. M. Feliu. Effect of adatoms in the electrocatalysis of HCOOH oxidation. A theoretical model. *Langmuir* 13, pp. 6287-6293, 1997.
- [25] M. Macia, E. Herrero and J. Feliu. Formic acid oxidation on Bi/Pt (111) electrode in perchloric acid media. A kinetic study. *J Electroanal Chem* 554, pp. 25-34, 2003.
- [26] Y. Yang, S. Sun, Y. Gu, Z. Zhou and C. Zhen. Surface modification and electrocatalytic properties of Pt (100), Pt (110), Pt (320) and Pt (331) electrodes with Sb towards HCOOH oxidation. *Electrochim. Acta* 46, pp. 4339-4348, 2001.
- [27] W. Sangarunlert, S. Sukchai, A. Pongtornkulpanich, A. Nathakaranakule and T. Lushtinetz. Technical and economic evaluation of a formic acid/hydrogen peroxide fuel cell system with Pt-M/C as anode catalyst. *Journal of Fuel Cell Science and Technology* 8, pp. 061005, 2011.
- [28] G. Saravanan, K. Nanba, G. Kobayashi and F. Matsumoto. Leaching tolerance of anodic Pt-based intermetallic catalysts for formic acid oxidation. *Electrochim. Acta* 99, pp. 15-21, 2013.

- [29] R. B. Moghaddam, O. Y. Ali, M. Javashi, P. L. Warburton and P. G. Pickup. The effects of conducting polymers on formic acid oxidation at Pt nanoparticles. *Electrochim. Acta* 162, pp. 230-236, 2014.
- [30] R. B. Moghaddam and P. G. Pickup. Oxidation of formic acid at polycarbazole-supported Pt nanoparticles. *Electrochim. Acta* 97, pp. 326-332, 2013.
- [31] A. Malinauskas. Electrocatalysis at conducting polymers. *Synth Met* 107, pp. 75-83, 1999.

CHAPTER 5

Summary and Future Work

5 Summary and Future Work

Drop coated Pt (Pt NP) on GC electrodes modified by Sb via a solution immersion method are shown to produce powerful electrocatalysts for formic acid oxidation. GC/Pt-Sb electrocatalysts have shown an improvement of 50 times in the electroactivity for formic acid oxidation relative to a GC/Pt electrode. They have also shown significant improvement in the onset potential of formic acid oxidation (+100 mV for GC/Pt, -50 mV for GC/Pt-Sb). The maximum achievable coverage of Sb onto Pt was found to be about 33% and the coverage (%) versus electroactivity has been found to be linearly correlated. Chronoamperometric studies at constant potential for GC/Pt-Sb showed an improved resistance to poisoning (formation of CO) relative to GC/Pt.

The presence of Bi ad-atoms increases the Pt activity via a third body effect (impeding poisoning of Pt by CO) and possibly by an electronic effect and the difference in the catalytic activity of Bi modified Pt relative to Pt was roughly 80 times for oxidation of formic acid in an acidic medium (0.1 M H₂SO₄). There was a linear relationship between the immersion time and adsorption of Bi on the surface of the Pt. There was a linear correlation between the electroactivity for formic acid oxidation and coverage (%) of Bi ad-atoms on the Pt. The optimum time for immersion was found to be 40 min and the optimum concentration of the metal solution for deposition was found to be 0.1 mM Bi₂O₃ for 0.1 M H₂SO₄ solutions. Also the acid solution molarity plays a critical role for deposition. Therefore, the deposition time, pH and concentration of metal solution are key factors for the solution deposition method. The stability of the ad-atoms of Bi was also evaluated and it

was found that the stability of ad-atoms is highly dependent on the applied positive potential limit and the positive potential limit should not be more than 550 mV vs. SCE in order to avoid desorption.

Polymer supports have been found to play a very positive role for the enhancement of the electroactivity of Pt electrocatalysts for formic acid oxidation and PANI improved both the onset potential as well as the peak current for formic acid oxidation when used with Pt. However, in the case of Bi ad-atom modified Pt, PANI only showed an increase in the peak current for formic acid oxidation.

As far as future work is concerned, the major issue that needs to be dealt with is the stability of the irreversibly adsorbed ad-atoms (Sb, Bi). There is a need to find a way to stop the leaching of adsorbed ad-atoms. This may be achieved by making NP containing both Pt and ad-atoms (Sb, Bi), or core-shell NP with either the core or shell with any one or both Sb and Bi. Probably, we could stop leaching of adsorbed ad-atoms by coating Pt/Bi or Pt/Sb by a thin layer of polymers like PANI or polycarbazole.